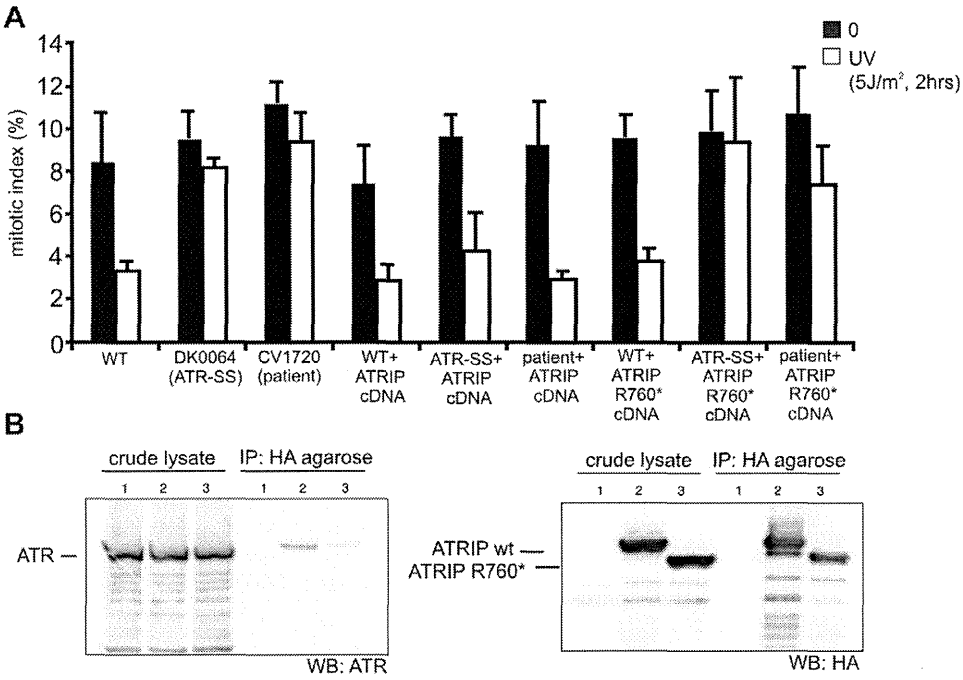

Figure 3. WT ATRIP cDNA but not cDNA encoding p.Arg760* ATRIP complements the G2/M checkpoint defect in CV1720 cells, and p.Arg760*ATRIP impairs ATR–ATRIP protein interaction. A) Analysis of the G2/M checkpoint defect in CV1720 cells following expression of ATRIP cDNA. G2/M checkpoint arrest was examined 2 h post exposure to 5 Jm^{-2} UV. As shown in Figure 1A, WT cells showed proficient checkpoint arrest whilst DK0064 (ATR–SS) and CV1720 (patient) cells are unable to undergo arrest. Expression of WT ATRIP cDNA restored the ability of CV1720 (patient) and DK0064 (ATR–SS) to undergo checkpoint arrest but this was not observed following transfection of cDNA encoding R760* ATRIP. Significantly, expression of ATRIP R760* did not impair checkpoint arrest in WT cells verifying that it does not exert a dominant negative impact. Results represent the mean and SD of three experiments. WT cells were GM2188. ATR–SS represents DK0064 and patient, CV1720. B) R760* ATRIP impairs ATR–ATRIP interaction. Crude lysates were prepared from HEK293T cells and either mock transfected (lane1), transfected with HA-tagged WT *ATRIP* cDNA (lane2), or R760* *ATRIP* cDNA (lane3) (generating p.Arg760* ATRIP protein) together with *ATR* cDNA. The extracts were immunoprecipitated with agarose-conjugated rabbit anti-HA-tag antibody (MBL). Interaction with ATR was examined by immunoblotting with ATR antibodies (left panel). Immunoblotting using the HA-tag (ATRIP; right panel) verified expression of the appropriately sized ATRIP in the samples. 33% of the crude lysate was loaded; IP, immunoprecipitate.
doi:10.1371/journal.pgen.1002945.g003

(ATR–SS) cells (Figure 5A) [7]. Checkpoint arrest after exposure to ionising radiation was activated normally. Additionally, we examined the phosphorylation of a range of ATR substrates following exposure to 0.5 mM HU and observed impaired phosphorylation in both 27-4BI and 19-8BI cells (Figure 5B). Collectively, these functional data substantiate a deficiency in the ATR–dependent DNA damage response in LBLs from these two cases. Thus, we conclude that both patients represent further ATR–SS patients.

Discussion

Although the first causal defect for SS was identified as ATR in 2003, further patients with mutations in *ATR* have not been reported [7]. SS patients are characterised by microcephaly and growth delay, features also observed in other microcephalic, primordial dwarfism syndromes including MOPD type II and MGS. Given that all ATR–SS patients to date share consanguinity, there are limitations in defining the spectrum of clinical features conferred by ATR deficiency to support a clinical distinction between ATR–SS and related disorders such as MOPD type II and MGS as well as other sub-classes of SS [1–3,31].

Here, we describe the novel identification of a patient mutated in ATRIP, the binding partner of ATR. Thus, we identify *ATRIP* as a new causal gene for SS. The mutational change in one *ATRIP* allele lies within a region previously suggested to be required for interaction with ATR, which is consolidated by our work [21,30]. We demonstrate that the second allele is abnormally spliced causing a reduction in *ATRIP* mRNA from that allele. qRT-PCR analysis suggested that there could be 25% residual WT *ATRIP* expressed in the patient cells. Consistent with this, we routinely observed ~10–20% of WT ATRIP protein in CV1720 cells by Western Blotting, although the level was variable between preparations. Although not examined in detail, there appeared to be a correlation between proliferation status and ATRIP levels, with the levels decreasing as proliferation slowed. Thus, differences in the proliferative state of cells at the time of analysis may underlie the apparent difference between Western Blotting and qRT-PCR analysis. Notwithstanding some limitations in quantification, the patient clinical features were marked despite ~10–20% residual ATRIP expression. Similarly, in patient DK0064, residual ATR protein can be readily detected [7]. Thus, we conclude that reduced but detectable levels of ATR/ATRIP protein can confer a clinical phenotype.

Additionally, we identify two further SS patients with ATR mutations in two unrelated families native to the UK. Interestingly, despite being unrelated, 27-4BI and 19-8BI carry the same compound heterozygous mutations, possibly representing founder mutations in the UK population.

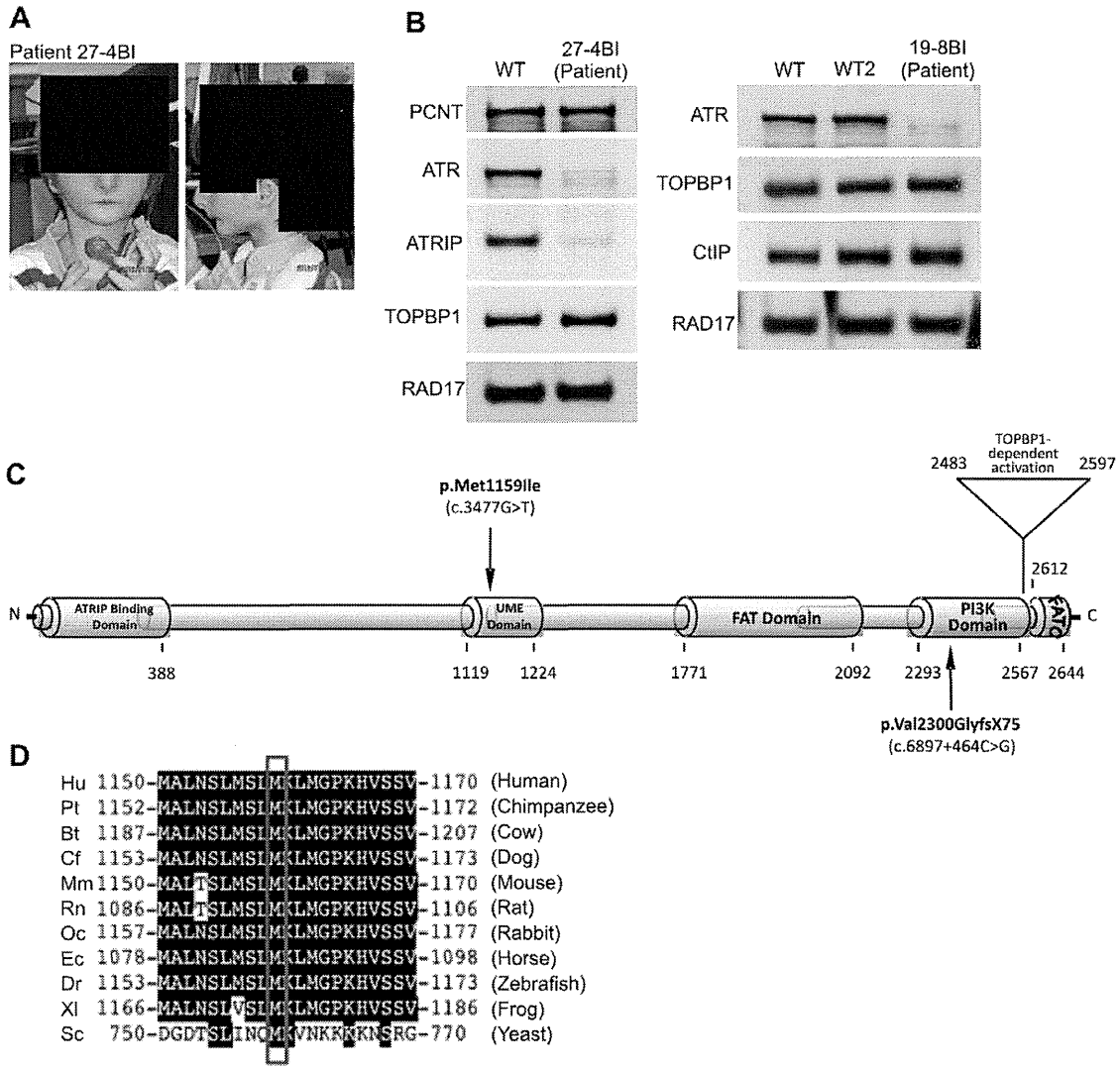

Figure 4. Patients 27-4BI and 19-8BI have reduced ATR and ATRIP expression and mutations in ATR. A) Photographs of patient included with informed consent of parent. B) Cell extracts (50 μg) from LBLs derived from WT (IM257), patient 27-4BI or patient 19-8BI were immunoblotted using the indicated antibodies. Reduced expression of ATR was observed in both patients. 27-4BI also had reduced ATRIP expression. C) Structure of ATR showing the site of the mutations identified and the UME domain. D) The UME domain is conserved between species and the methionine residue within this domain is conserved in yeast.
doi:10.1371/journal.pgen.1002945.g004

All four ATR/ATRIP patients displayed severe microcephaly and growth delay (Table 1). All patients also displayed micrognathia, receding forehead, dental crowding and microtia with small or absent lobes (Figure 4A). Interestingly, an MRI scan of the ATRIP–SS patient revealed an abnormally small pituitary with absent fossa, which could contribute to the delayed growth observed (Figure S1). In distinction to the original ATR–SS patient (DK0064), patients 27-4BI and 19-8BI showed more marked skeletal abnormalities including digital features and aberrant patellae suggesting that ATR deficiency can have a detrimental impact on bone development (Table 1, Figure S4) [32]. Interestingly, aberrant patellae is a clinical feature commonly exhibited by MGS patients suggestive of a biological overlap between the ATR checkpoint pathway and the replication machinery during skeletal development and maintenance. In keeping with this, characterisation of a mouse model harbouring the same mutational change identified in the original ATR–SS patient (DK0064) revealed marked bone abnormalities including kyphosis and osteoporosis [32]. Our findings suggest that ATR–ATRIP SS shows more overlap with MGS than previously recognised (Table 2). However, whereas ATR–ATRIP SS patients tend to have very marked microcephaly, growth delay, dental crowding, small ears and less severe skeletal abnormalities, the spectrum for MGS tends to be less marked microcephaly and growth delay but a striking impact on skeletal development. Nonetheless, there does not appear to be an absolute clinical divide between these two disorders. Significantly, these overlapping clinical features could reflect the fact that both ATR/ATRIP

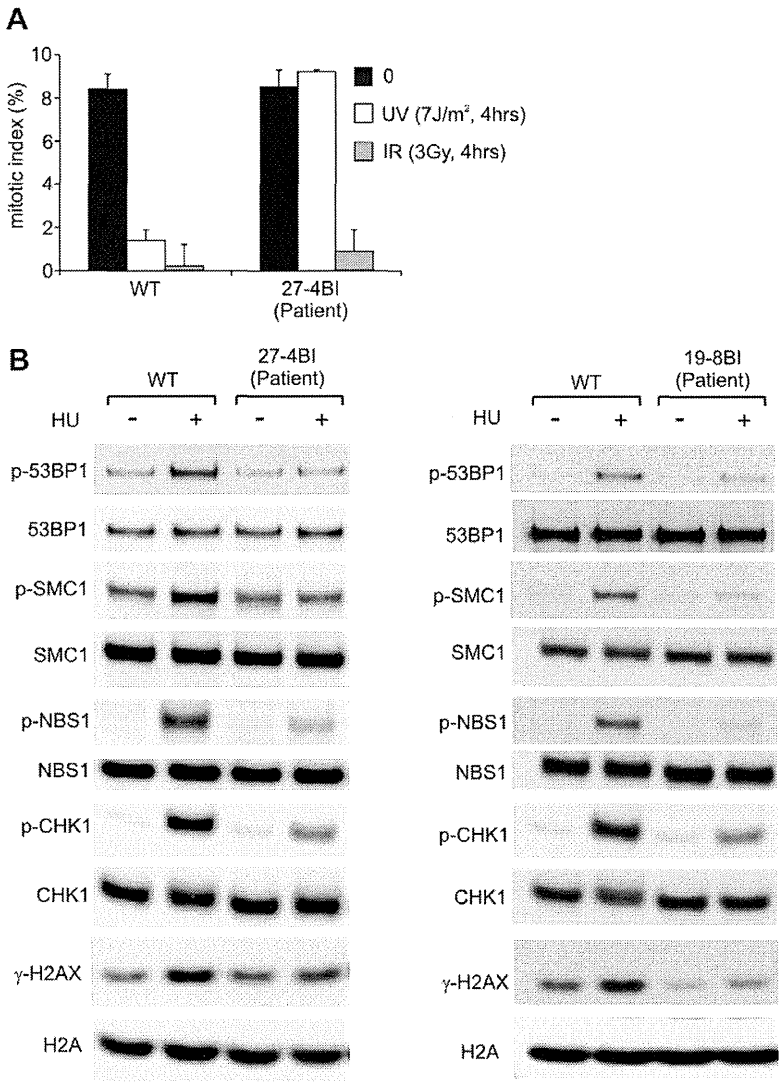

Figure 5. LBLs from patient 27-4BI and 19-8BI showed impaired ATR–dependent damage responses. A) 27-4BI cells were examined for their ability to activate G2/M checkpoint arrest at 4 h following exposure to 7 Jm^{-2} UV. In contrast to WT cells (GM2188), no significant arrest was observed in 27-4BI cells. The checkpoint response to ionizing radiation, which is ATM rather than ATR dependent, was normal. B) LBLs derived from patients 27-4BI and 19-8BI were examined for their ability to phosphorylate the indicated ATR substrates at 1 h following exposure to 0.5 mM HU. WT represents IM257. 27-4BI and control LBLs have a similar cell cycle profile demonstrating that the lack of ATR substrate phosphorylation cannot be attributed to the lack of S phase cells (Figure S2).
doi:10.1371/journal.pgen.1002945.g005

and the origin licensing complex play an essential role in promoting efficient replication and recovery from fork stalling, which may be vital during developmental stages involving rapid replication [13].

In summary, we provide the first report of a SS patient with mutations in *ATRIP*, defining a further novel genetic defect for this disorder, and describe two additional patients native to the UK, with mutations in *ATR*. The description of multiple ATR–ATRIP patients allows us to define a spectrum of clinical features conferred by *ATR–ATRIP* mutations. The clinical characteristics include severe microcephaly and growth delay, small or absent ear lobes, micrognathia and dental crowding. In addition, the novel ATR–mutated cases described here expand the clinical impact of impaired ATR–function to include more marked skeletal involvement.

Methods

Ethics Statement

Ethical approval for the research was granted by the School of Life Sciences Research Governance Committee, University of Sussex. Informed consent was obtained and clinical investigations were conducted according to the principles expressed in the Declaration of Helsinki. Patient material was gathered under conditions of the Human Tissue Authority (HTA licence number 12119).

Patients and cell lines

CV1720 is a SS patient of Gujarati-Indian origin. Patients 27-4BI and 19-8BI are English. The clinical features are described in

Table 2. MGS and Seckel syndrome patient phenotypes.

	ORC1 - MGS	Pre-RC MGS	ATR/ATRIP SS
Number of patients	10	25	4
OFC (cm)*	−5.4 to −11 SD	+1.7 to −5.0 SD	−10 to −12 SD
Height (cm)*	−4.5 to −9.6 SD	−0.4 to −6.4 SD	−5 to −8 SD
Weight (kg)*	0.8 to −11 SD	−0.3 to −9.9 SD	−3.3 to −8 SD
Intellectual disability	Ranges from none to mild/moderate	None	Developmental delay (2/4)
Facial Features	Small and abnormal ears (9/10), micrognathia (5/10), down slanted palpebral fissures (1/10)	Small and abnormal ears(25/25), micrognathia (20/25), down slanted palpebral fissures (8/25)	Small and/or abnormal ears (4/4), micrognathia (4/4), receding forehead (4/4), prominent nose (4/4), short palpebral fissures (2/4)
Skeletal abnormalities	Delayed bone age (3/10), Slender long bones (2/10) , absent patellae (6/10), genu recurvatum (4/10)	Delayed bone age (11/25), slender long bones, absent patellae (24/25)	Delayed bone age (1/4), 5th finger clinodactyly (2/4), symmetric dwarfism (3/4), small/abnormal patellae (2/4), kyphosis (1/4), hip abnormality (2/4), narrow pelvis (iliac blades) (1/4)
MRI	Normal in 2 patients examined	NA	Generalised cerebral atrophy, delayed myelination, abnormal gyration (2 patients examined)
Other	High pitched voice (1/10), full lips (7/10), cryptochordism (2/4 examined), mammary hypoplasia (2/2 examined), feeding and respiratory problems during infancy (8/10)	Full lips (14/25), cryptochordism (7/14 examined), mammary hypoplasia (8/8 examined), feeding (20/25) and respiratory (9/25) problems during infancy	Dental crowding (4/4), feeding and respiratory problems during infancy (1/4)

*standard deviations from the age-related normal population mean, NA = not assessed.
MGS data from [13,14] [33,34].
doi:10.1371/journal.pgen.1002945.t002

Table 1. Lymphoblastoid cell lines (LBLs) were derived from blood following EBV transformation. WT LBLs were GM2188 or LB197 as indicated. All LBLs were grown in RPMI medium supplemented with 10% foetal calf serum, penicillin, and streptomycin. Transfection with *ATRIP* cDNA was with Genejuice Transfection Reagent (Novagen, Merck Millipore, UK) following the manufacturers protocol.

qRT–PCR. Transcript levels of the *ATRIP*–c.2278C (normal) and *ATRIP*–c.2278C>T (p.Arg760*) alleles in LBLs from patient CV1720, and the parents were determined by the cycleave quantitative real time PCR (Cycleave-qPCR, TaKaRa Co. Ltd, Kyoto Japan) as well as standard site specific q-PCR (carried out in triplicate). Transcripts from the *HPRT1* allele were used as a quantification control. In the Cycleave qPCR, RNaseH sensitive fluorescent probes that specifically recognize the c.2278C and c.2278C>T alleles were used for the assay. qPCR results were analyzed by the ΔΔCT method. qPCR primers and probes used for the assay are listed below. (172F, 5′-CTTCACTGCCGACGACCTGG-3′; 191R, 5′-TTTGCTCGTTCACTGGTCTG-3′; P1, 5′-GGGGTCAGCATGCTCATCC-3′; P2, 5′-GGGGGTCAGCATGCTCATCT-3′; P3C, 5′-ACCTCGGGGTCTTCCACATC-3′; P4, 5′- -3′; P5, 5′- -3′; P6C, 5′- -3′; P7, 5′-GCCTATCGCAGAAGGACAAG-3′; P8, 5′-GGGTCTTCCACATCGGTTTC-3′; probe1 for c.2278C, 5′Eclipse-CCCTC(rG)GAT-3′FAM; probe2 for c.2278C, 5′Eclipse- GCCCTC(rA)GA-3′ROX)

Co-immunoprecipitation. To investigate the interaction of the ATRIP proteins with ATR, HEK293T cells were transfected with the HA-tagged *ATRIP* cDNA expressing plasmids (wild type and 2278C>T *ATRIP*) together with *ATR* cDNA, followed by 24 h incubation. Whole cell lysates were prepared using CelLytic Nuclear Extraction Kit (Sigma, St. Louis). Co-immunoprecipitation was performed using rabbit anti-HA antibody-conjugated agarose beads (MBL, Nagoya, Japan). Western blotting was carried out using ATR or anti-HA (detecting HA-tagged ATRIP) antibodies. Anti-ATR was N19 (Santa Cruz, Santa Cruz) at 1:200 dilution. Anti-HA-tag antibody, 132-3 (MBL, Nagoya, Japan), was used at 1:1000 dilution.

Immunofluorescence for analysis of γH2AX and 53BP1 staining

Cells were cytospun onto slides, fixed with 3% formaldehyde for 10 min and permeabilized in 0.5% Triton-X100. After antibody treatment and staining with 4,6-diamidino-2-phenylindole (DAPI), coverslips were mounted in Vectashield mounting medium (Vector Laboratories, Burlingame). Samples were incubated with primary antibodies for γ-H2AX (Millipore, Billerica) or 53BP1 (Bethyl, Montgomery). Secondary antibodies were from Sigma (St. Louis).

Western blotting

Cells were lysed for one hour in IPLB (50 mM Tris-HCl, 150 mM NaCl, 2 mM EDTA, 2 mM EGTA, 25 mM NaF, 25 mM β-glycerolphosphate, 0.1 mM NaOrthovanadate, 0.2% Triton X-100, 0.3% NP-40, plus protease inhibitor cocktail (Roche, Basel) at 4°C, centrifuged at 13,000 rpm for 10 minutes. The soluble fraction was subjected to SDS-PAGE and transferred to a nitrocellulose membrane for protein detection.

Antibodies raised against ATR, CHK1 (FL476) and MCM2 (N19) were from Santa Cruz (Santa Cruz). Anti-FANCD2, ATRIP and phospho-Chk1 (Ser317) antibodies were from Novus (Littleton), Bethyl (Montgomery), and Cell Signaling (Beverly, Woburn), respectively.

G2/M checkpoint arrest

Cells were exposed to 5 or 7 Jm^{-2} UV, or 3Gy ionising radiation and incubated for 2 or 4 hours (as indicated) in complete medium containing 0.2 ug/ml Colcemid (Invitrogen, Carlsbad), followed by processing for immunofluorescence as detailed above. Mitotic cells were detected by α-Histone H3-pSer10 antibodies (Millipore, Billerica) and cells were counterstained with DAPI.

Supporting Information

Figure S1 Photograph of limbs and MRI scan of patient CV1720. Left hand photograph showing hands and feet. Right hand photograph shows an MRI scan where a small pituitary is evident.
(TIF)

Figure S2 Cell cycle analysis of WT, DK0064 (ATR–SS), 27-4BI, and CV1720 patient LBLs. A) Asynchronous growing cultures of WT, DK0064 (ATR–SS), 27-4BI and CV1720 patient cells were pelleted, fixed in 70% ice-cold ethanol and stained with propidium iodide prior to FACs analysis. Populations were gated and the proportion of cells in G1, S and G2/M phases of the cell cycle measured. B) WT, DK0064 (ATR–SS), 27-4BI and CV1720 patient cells were treated with nocodazole for 16 h and then fixed and analysed as in a). C) Asynchronous growing cultures of WT, DK0064 (ATR–SS), 27-4BI and CV1720 patient cells were pulse-labelled with 50 μM BrdU for 1 h. Cells were then fixed in 70% ice-cold ethanol and processed for BrdU FACs analysis as described in Bicknell et al, 2011 [13]. The proportion of cells in S phase were gated and measured. Each graph represents the mean of three independent experiments. The error bars represent the standard deviation.
(TIF)

Figure S3 Identification of a truncating mutation in *ATRIP* in patient, CV1720. Genomic DNA sequencing of *ATRIP* exons showed that patient CV1720 and the unaffected mother, CV1780, are heterozygous for a c.2278C>T mutational change in exon12 of *ATRIP*. The father has a WT sequence at this site. 2278C>T generates a primary stop codon predicting a truncated protein at position arginine 760 (p.R760*). WT sequence shown in blue, the mutation is shown in Red.
(TIF)

Figure S4 Photographs of patients 27-4BI and 19-8BI. A) Shows abnormal digits of patient 27-4BI. B) Copper beaten appearance of skull of patient 19-8BI. C) Frontal and Lateral view of left knee of patient 19-8BI showing an absence of ossification of the patella.
(TIF)

Figure S5 Mutational changes observed in *ATR* in patients 27-4BI and 19-8BI. A) c.3477G>T mutational change in patients 27-4BI and 19-8BI. RT-PCR sequencing revealed a heterozygous 3477G>T mutational change in both patients causing an amino acid substitution, p.Met1159Ile, which lies within a conserved UME (NUC010) domain of ATR. B) A double sequence was observed at the boundary between exons 40 and 41 in both patients. Sequencing showed that the double sequence was caused by insertion of a 142 bp region from intron 40. C) A C to G mutational change was observed in intron 41 of both patients converting the sequence CAGCT to CAGGT, a splice site. The insertion causes a frameshift and a stop codon at p.Val2300-Glyfs*75. D) Diagram showing the likely origin of the insertion observed at the exon 40/41 boundary. Sequencing of intron 40 revealed a C>G mutation as indicated creating a cryptic splice site causing splicing of exon 40 to the indicated intronic sequence (which represents an Alu repeat sequence). Thus one ATR allele of the patients harbours a 142 nucleotide insertion between exons 40 and 41. Exons 40 and 41 are highlighted in green and the inserted intronic sequence is shown in red. The intronic C>G change is highlighted in red. The insertion causes a frameshift and a stop codon at c.6978 in exon 41.
(TIF)

Table S1 The table shows the position of single nucleotide polymorphisms identified in intron 1 and 2 in the patient and parental genomic DNA. * The contig position is defined as the position of the single nucleotide variant (SNV) on the contig (NT_022517.17) when counting from the first base (base position = 1). **rs# is the NCBI's reference SNP ID. *** minor allele (indicated as a base) and its frequency (MAF) (second most frequent allele) in a default global population reported in dbSNP database (1000 Genome phase 1, May 2011). N.A. not available.
(DOCX)

Acknowledgments

We thank Dr. E. Riballo and P. Gajwani for contributions to this work and Dr. D. Cortez for providing *ATRIP* cDNA.

Author Contributions

Conceived and designed the experiments: TO GSS AMRT MO PAJ. Performed the experiments: SW TS SL GC MM NM YN. Analyzed the data: TO TS GSS AMRT MO PAJ. Contributed reagents/materials/analysis tools: EH KP MS PJB PV MB. Wrote the paper: PAJ. Aided in writing the paper: MO GSS TO AMRT.

References

1. Majewski F, Goecke T (1982) Studies of microcephalic primordial dwarfism I: approach to a delineation of the Seckel syndrome. Am J Med Genet 12: 7–21.
2. Hall JG, Flora C, Scott CI, Jr., Pauli RM, Tanaka KI (2004) Majewski osteodysplastic primordial dwarfism type II (MOPD II): natural history and clinical findings. Am J Med Genet A 130: 55–72.
3. Gorlin RJ (1992) Microtia, absent patellae, short stature, micrognathia syndrome. J Med Genet 29: 516–517.
4. Thornton GK, Woods CG (2009) Primary microcephaly: do all roads lead to Rome? Trends Genet 25: 501–510.
5. Goodship J, Gill H, Carter J, Jackson A, Splitt M, et al. (2000) Autozygosity mapping of a seckel syndrome locus to chromosome 3q22. 1-q24. Am J Hum Genet 67: 498–503.
6. Borglum AD, Balslev T, Haagerup A, Birkebaek N, Binderup H, et al. (2001) A new locus for Seckel syndrome on chromosome 18p11.31-q11.2. Eur J Hum Genet 9: 753–757.
7. O'Driscoll M, Ruiz-Perez VL, Woods CG, Jeggo PA, Goodship JA (2003) A splicing mutation affecting expression of ataxia-telangiectasia and Rad3-related protein (ATR) results in Seckel syndrome. Nature Genetics 33: 497–501.
8. Qvist P, Huertas P, Jimeno S, Nyegaard M, Hassan MJ, et al. (2011) CtIP Mutations Cause Seckel and Jawad Syndromes. PLoS Genet 7: e1002310. doi:10.1371/journal.pgen.1002310
9. Al-Dosari MS, Shaheen R, Colak D, Alkuraya FS (2010) Novel CENPJ mutation causes Seckel syndrome. J Med Genet 47: 411–414.
10. Kalay E, Yigit G, Aslan Y, Brown KE, Pohl E, et al. (2011) CEP152 is a genome maintenance protein disrupted in Seckel syndrome. Nat Genet 43: 23–26.
11. Griffith E, Walker S, Martin CA, Vagnarelli P, Stiff T, et al. (2008) Mutations in pericentrin cause Seckel syndrome with defective ATR–dependent DNA damage signaling. Nat Genet 40: 232–236.
12. Rauch A, Thiel CT, Schindler D, Wick U, Crow YJ, et al. (2008) Mutations in the pericentrin (PCNT) gene cause primordial dwarfism. Science 319: 816–819.
13. Bicknell LS, Walker S, Klingseisen A, Stiff T, Leitch A, et al. (2011) Mutations in ORC1, encoding the largest subunit of the origin recognition complex, cause microcephalic primordial dwarfism resembling Meier-Gorlin syndrome. Nat Genet 43: 350–355.
14. Bicknell LS, Bongers EM, Leitch A, Brown S, Schoots J, et al. (2011) Mutations in the pre-replication complex cause Meier-Gorlin syndrome. Nat Genet 43: 356–359.
15. Willems M, Genevieve D, Borck G, Baumann C, Baujat G, et al. (2010) Molecular analysis of pericentrin gene (PCNT) in a series of 24 Seckel/microcephalic osteodysplastic primordial dwarfism type II (MOPD II) families. Journal of medical genetics 47: 797–802.
16. Nam EA, Cortez D (2011) ATR signalling: more than meeting at the fork. The Biochemical journal 436: 527–536.
17. Zou L, Elledge SJ (2003) Sensing DNA damage through ATRIP recognition of RPA-ssDNA complexes. Science 300: 1542–1548.
18. Ciccia A, Elledge SJ (2010) The DNA damage response: making it safe to play with knives. Mol Cell 40: 179–204.

19. Cortez D, Guntuku S, Qin J, Elledge SJ (2001) ATR and ATRIP: partners in checkpoint signaling. Science 294: 1713–1716.
20. Namiki Y, Zou L (2006) ATRIP associates with replication protein A-coated ssDNA through multiple interactions. Proceedings of the National Academy of Sciences of the United States of America 103: 580–585.
21. Ball HL, Myers JS, Cortez D (2005) ATRIP binding to replication protein A-single-stranded DNA promotes ATR–ATRIP localization but is dispensable for Chk1 phosphorylation. Molecular biology of the cell 16: 2372–2381.
22. Paciotti V, Clerici M, Lucchini G, Longhese MP (2000) The checkpoint protein Ddc2, functionally related to S. pombe Rad26, interacts with Mec1 and is regulated by Mec1-dependent phosphorylation in budding yeast. Genes Dev 14: 2046–2059.
23. Lakin ND, Jackson SP (1999) Regulation of p53 in response to DNA damage. Oncogene 18: 7644–7655.
24. Ward IM, Chen J (2001) Histone H2AX is phosphorylated in an ATR-dependent manner in response to replicational stress. J Biol Chem 276: 47759–47762.
25. Alderton GK, Joenje H, Varon R, Borglum AD, Jeggo PA, et al. (2004) Seckel syndrome exhibits cellular features demonstrating defects in the ATR signalling pathway. Human Molecular Genetics 13: 3127–3138.
26. Toledo LI, Murga M, Zur R, Soria R, Rodriguez A, et al. (2011) A cell-based screen identifies ATR inhibitors with synthetic lethal properties for cancer-associated mutations. Nature structural & molecular biology 18: 721–727.
27. Chanoux RA, Yin B, Urtishak KA, Asare A, Bassing CH, et al. (2009) ATR and H2AX cooperate in maintaining genome stability under replication stress. The Journal of biological chemistry 284: 5994–6003.
28. Andreassen PR, D'Andrea AD, Taniguchi T (2004) ATR couples FANCD2 monoubiquitination to the DNA damage response. Genes and Development 18: 1958–1963.
29. Noensie EN, Dietz HC (2001) A strategy for disease gene identification through nonsense-mediated mRNA decay inhibition. Nature biotechnology 19: 434–439.
30. Falck J, Coates J, Jackson SP (2005) Conserved modes of recruitment of ATM, ATR and DNA-PKcs to sites of DNA damage. Nature 434: 605–611.
31. Klingseisen A, Jackson AP (2011) Mechanisms and pathways of growth failure in primordial dwarfism. Genes & development 25: 2011–2024.
32. Murga M, Bunting S, Montana MF, Soria R, Mulero F, et al. (2009) A mouse model of ATR–Seckel shows embryonic replicative stress and accelerated aging. Nature genetics 41: 891–898.
33. Guernsey DL, Matsuoka M, Jiang H, Evans S, Macgillivray C, et al. (2011) Mutations in origin recognition complex gene ORC4 cause Meier-Gorlin syndrome. Nat Genet 43: 360–364.
34. de Munnik SA, Bicknell LS, Aftimos S, Al-Aama JY, van Bever Y, et al. (2012) Meier-Gorlin syndrome genotype-phenotype studies: 35 individuals with pre-replication complex gene mutations and 10 without molecular diagnosis. European journal of human genetics : EJHG 20: 598–606.

Journal of Human Genetics (2014), 1–2

www.nature.com/jhg

COMMENTARY

A commentary on the promise of whole-exome sequencing in medical genetics

Tadashi Kaname, Kumiko Yanagi and Kenji Naritomi

Journal of Human Genetics advance online publication, 6 February 2014; doi:10.1038/jhg.2014.7

The dawn of next-generation sequencers (NGSs) and innovative sequencing technologies have brought a paradigm shift in medical research and clinical practice. Furthermore, the cost reduction of NGSs enables personalized medicine to come to fruition.

However, whole-genome sequencing (WGS) remains expensive when applied to personal genome analysis. WGS generates a large amount of data that requires high-performance computer processing. Targeted whole-exon capture and sequencing [whole-exome sequencing (WES)] is more cost-effective when compared with WGS because exons represent only ~1–2% of the genome and also higher sequence coverage can be achieved by NGSs. In addition, most Mendelian disorders are caused by exonic mutations or splice-junction mutations, and protein-coding genes harbor ~85% of the mutations that have large effects on disease-related traits.[1] Thus, WES will provide many advantages and lower costs than WGS when analyzing personal genomes.

WES was first successfully used in 2010 to discover the gene responsible for Miller syndrome, a Mendelian disorder.[2] Since then, WES has been increasingly used as a fast and accurate genomic discovery approach to investigate both rare genetic disorders and common diseases.

WES is widely applied across different areas of medicine, because it has the added advantage of reduced cost and requires analysis of a much smaller but essential dataset when compared with WGS. In addition, recent clinical molecular diagnostics have used WES to detect heterogeneous Mendelian diseases.[3,4]

A recent review of WES approaches in medical genetics describes the usefulness of WES in medicine and medical research and the impact of WES on clinical diagnoses.[5] WES approaches have greatly facilitated the discovery of candidate genes or gene variants in Mendelian disorders and rare variants in common diseases and genomic characterization in cancer. Currently, WES is increasingly being applied to disease gene discovery, cancer typing and molecular diagnosis.[5]

Presently, WES is an essential tool in medical genetics, especially in the research of Mendelian disorders. WES or multigene tests using NGSs are widely applied to heterogeneous disorders including deafness or ciliopathy.[5,6] WES is also being increasingly applied to genetic testing for undiagnosed patients.[4,5] Yang *et al.*[4] performed WES in undiagnosed patients whose phenotypes were suggestive of potential genetic disorders and achieved a molecular diagnosis for 62 of 250 (25%) patients.

Because WES detects individual genetic variation, it can be used to construct a variation database of anthropic and ethnic populations. At the same time, because WES can detect groups of genetic variations that are unrelated to the indication for the first diagnostic purpose but are of medical value for individual patient care, such 'incidental findings' pose potential ethical problems that should be strongly considered and discussed in clinical practice.[5,7]

WES is a widely applied technique in medical genetics that is capable of detecting variations in whole exons. However, in practical use, understanding WES methodology and limitations are important. Current WES techniques are not capable of detecting all of the variations surrounding exons. Detecting variation by WES is limited by the experimental methods, probe coverage and/or platforms used.[8–10] Hence, WES may not always detect pathogenic or causative variations in a genetic disease. In addition, because WES is a method to detect genomic sequence variations, when a candidate of causative variation in the disease is detected, it requires verification or support by secondary analyses. In particular, further functional analyses are important to confirm whether the variant is pathogenic or benign.

Nevertheless, WES enables the unprecedented low cost and highly efficient analysis of whole exons. WES can be easily used to comprehensively detect individual variations in exons. It is without doubt that WES is a powerful tool in genome analysis, and it greatly progresses medical genetics.

Although WESs' limitations need to be overcome, we anticipate that WES will be used not only in medical research but also in clinical practice for example, molecular diagnosis (whole-gene test) and personal genomics before WGS becomes a common place in medical genetics. Thus, a paradigm shift in medicine by advancement in both WES and WGS is expected to continue.

T Kaname, K Yanagi and K Naritomi are at Department of Medical Genetics, University of the Ryukyus Graduate School of Medicine, Okinawa, Japan
E-mail: tkaname@med.u-ryukyu.ac.jp

1 Majewski, J., Schwartzentruber, J., Lalonde, E., Montpetit, A. & Jabado, N. What can exome sequencing do for you? *J. Med. Genet.* **48,** 580–589 (2011).
2 Ng, S. B., Buckingham, K. J., Lee, C., Bigham, A. W., Tabor, H. K., Dent, K. M. *et al.* Exome sequencing identifies the cause of a mendelian disorder. *Nat. Genet.* **42,** 30–35 (2010).
3 Kaname, T., Yanagi, K. & Naritomi, K. A commentary on the diagnostic utility of exome sequencing in Joubert syndrome and related disorders. *J. Hum. Genet.* **58,** 57 (2013).
4 Yang, Y., Muzny, D. M., Reid, J. G., Bainbridge, M. N., Willis, A., Ward, P. A. *et al.* Clinical whole-exome

sequencing for the diagnosis of Mendelian disorders. *N. Engl. J. Med.* **369,** 1502–1511 (2013).
5 Rabbani, B., Tekin, M. & Mahdieh, N. The promise of whole-exome sequencing in medical genetics. *J. Hum. Genet.* **59,** 5–15 (2014).
6 Tsurusaki, Y., Kobayashi, Y., Hisano, M., Ito, S., Doi, H., Nakashima, M. *et al.* The diagnostic utility of exome sequencing in Joubert syndrome and related disorders. *J. Hum. Genet.* **58,** 113–115 (2013).
7 Green, R. C., Berg, J. S., Grody, W. W., Kalia, S. S., Korf, B. R., Martin, C. L. *et al.* ACMG recommendations for reporting of incidental findings in clinical exome and genome sequencing. *Genet. Med.* **15,** 565–574 (2013).
8 Teer, J. K., Bonnycastle, L. L., Chines, P. S., Hansen, N. F., Aoyama, N., Swift, A. J. *et al.* Systematic comparison of three genomic enrichment methods for massively parallel DNA sequencing. *Genome Res.* **20,** 1420–1431 (2010).
9 Clark, M. J., Chen, R., Lam, H. Y., Karczewski, K. J., Chen, R., Euskirchen, G. *et al.* Performance comparison of exome DNA sequencing technologies. *Nat. Genet.* **29,** 908–914 (2011).
10 Wooderchak-Donahue, W. L., O'Fallon, B., Furtado, L. V., Durtschi, J. D., Plant, P., Ridge, P. G. *et al.* A direct comparison of next generation sequencing enrichment methods using an aortopathy gene panel- clinical diagnostics perspective. *BMC Med. Genomics* **5,** 50 (2012).

Malfunction of Nuclease ERCC1-XPF Results in Diverse Clinical Manifestations and Causes Cockayne Syndrome, Xeroderma Pigmentosum, and Fanconi Anemia

Kazuya Kashiyama,[1,2,3,16] Yuka Nakazawa,[2,4,16] Daniela T. Pilz,[5,16] Chaowan Guo,[2,4,16] Mayuko Shimada,[2,4] Kensaku Sasaki,[2,4] Heather Fawcett,[6] Jonathan F. Wing,[6] Susan O. Lewin,[7] Lucinda Carr,[8] Tao-Sheng Li,[9] Koh-ichiro Yoshiura,[10] Atsushi Utani,[11] Akiyoshi Hirano,[1] Shunichi Yamashita,[3,12] Danielle Greenblatt,[13] Tiziana Nardo,[14] Miria Stefanini,[14] David McGibbon,[13] Robert Sarkany,[13] Hiva Fassihi,[13] Yoshito Takahashi,[15] Yuji Nagayama,[4] Norisato Mitsutake,[2,3] Alan R. Lehmann,[6,17,*] and Tomoo Ogi[2,4,17,*]

Cockayne syndrome (CS) is a genetic disorder characterized by developmental abnormalities and photodermatosis resulting from the lack of transcription-coupled nucleotide excision repair, which is responsible for the removal of photodamage from actively transcribed genes. To date, all identified causative mutations for CS have been in the two known CS-associated genes, *ERCC8* (*CSA*) and *ERCC6* (*CSB*). For the rare combined xeroderma pigmentosum (XP) and CS phenotype, all identified mutations are in three of the XP-associated genes, *ERCC3* (*XPB*), *ERCC2* (*XPD*), and *ERCC5* (*XPG*). In a previous report, we identified several CS cases who did not have mutations in any of these genes. In this paper, we describe three CS individuals deficient in *ERCC1* or *ERCC4* (*XPF*). Remarkably, one of these individuals with XP complementation group F (XP-F) had clinical features of three different DNA-repair disorders—CS, XP, and Fanconi anemia (FA). Our results, together with those from Bogliolo et al., who describe XPF alterations resulting in FA alone, indicate a multifunctional role for XPF.

Cockayne syndrome (CS [MIM 216400 and 133540]) is a rare autosomal-recessive disorder characterized by growth retardation, microcephaly, impairment of nervous system development, pigmentary retinopathy, peculiar facies, and progeria together with abnormal skin photosensitivity.[1] On the basis of its clinical severity, CS is classified into three types: (1) CS type I, the classical (moderate) form, which is characterized by normal prenatal growth and the onset of progressive developmental abnormalities in infancy; (2) CS type II, the more severe (early-onset) form, in which prenatal developmental abnormalities are present; and (3) CS type III, a milder form in which progeroid symptoms manifest after middle age (see GeneReview in Web Resources). CS type II is often considered for differential diagnoses of other microcephalic maldevelopmental disorders, such as cerebrooculofacialskeletal syndrome (COFS [MIM 214150], also known as Pena-Shokeir syndrome type II) and Warburg Micro syndrome (MIM 600118).[2] In addition to these CS classes, there are rare CS variants that display the combined features of CS and XP (MIM 278700, 610651, 278720, 278730, 278740, 278760, and 278780), termed XPCS. Although CS is commonly associated with sunlight sensitivity, the dermatological phenotypes in CS are milder than those in XP and skin cancers are not found in CS. XPCS individuals, however, present with severe skin phenotypes, including severe photosensitivity, abnormal skin pigmentation, and skin cancer predisposition, all of which are common to XP individuals, who also show developmental abnormalities typical of CS.

XP and CS are associated with deficiencies in nucleotide excision repair (NER), which removes sunlight-induced UV photolesions and bulky DNA base adducts from cellular DNA.[3] NER is subdivided into two pathways, global genome NER (GG-NER) and transcription-coupled NER (TC-NER), which are distinct in their initial DNA-damage recognition processes. In contrast to XPCS, which causes defects in both pathways, CS causes specific defects to TC-NER.[4] To date, all CS (types I, II, and III)-affected individuals have been associated with mutations in *ERCC8*

[1]Department of Plastic and Reconstructive Surgery, Graduate School of Biomedical Sciences, Nagasaki University, 1-7-1 Sakamoto, Nagasaki 852-8501, Japan; [2]Nagasaki University Research Centre for Genomic Instability and Carcinogenesis, Nagasaki University, 1-12-4 Sakamoto, Nagasaki 852-8523, Japan; [3]Department of Radiation Medical Sciences, Atomic Bomb Disease Institute, Nagasaki University, 1-12-4 Sakamoto, Nagasaki 852-8523, Japan; [4]Department of Molecular Medicine, Atomic Bomb Disease Institute, Nagasaki University, 1-12-4 Sakamoto, Nagasaki 852-8523, Japan; [5]Institute of Medical Genetics, University Hospital of Wales, Cardiff CF14 4XW, UK; [6]Genome Damage and Stability Centre, University of Sussex, Falmer, Brighton BN1 9RQ, UK; [7]Division of Medical Genetics, Department of Pediatrics, University of Utah, Salt Lake City, UT 84132, USA; [8]Great Ormond Street Hospital for Children, London WC1N 3HJ, UK; [9]Department of Stem Cell Biology, Atomic Bomb Disease Institute, Nagasaki University, 1-12-4 Sakamoto, Nagasaki 852-8523, Japan; [10]Department of Human Genetics, Atomic Bomb Disease Institute, Nagasaki University, 1-12-4 Sakamoto, Nagasaki 852-8523, Japan; [11]Department of Dermatology, Graduate School of Biomedical Sciences, Nagasaki University, 1-12-4 Sakamoto, Nagasaki 852-8523, Japan; [12]Fukushima Medical University, Fukushima 960-1295, Japan; [13]UK National Xeroderma Pigmentosum Service, Department of Photodermatology, St. John's Institute of Dermatology, St. Thomas's Hospital, London SE1 7EH, UK; [14]Istituto di Genetica Molecolare, Consiglio Nazionale delle Ricerche, Pavia 27100, Italy; [15]Innovative Beauty Science Laboratory, Kanebo Cosmetics Inc., Odawara 250-0002, Japan
[16]These authors contributed equally to this work
[17]These authors contributed equally to this work
*Correspondence: togi@nagasaki-u.ac.jp (T.O.), a.r.lehmann@sussex.ac.uk (A.R.L.)
http://dx.doi.org/10.1016/j.ajhg.2013.04.007.

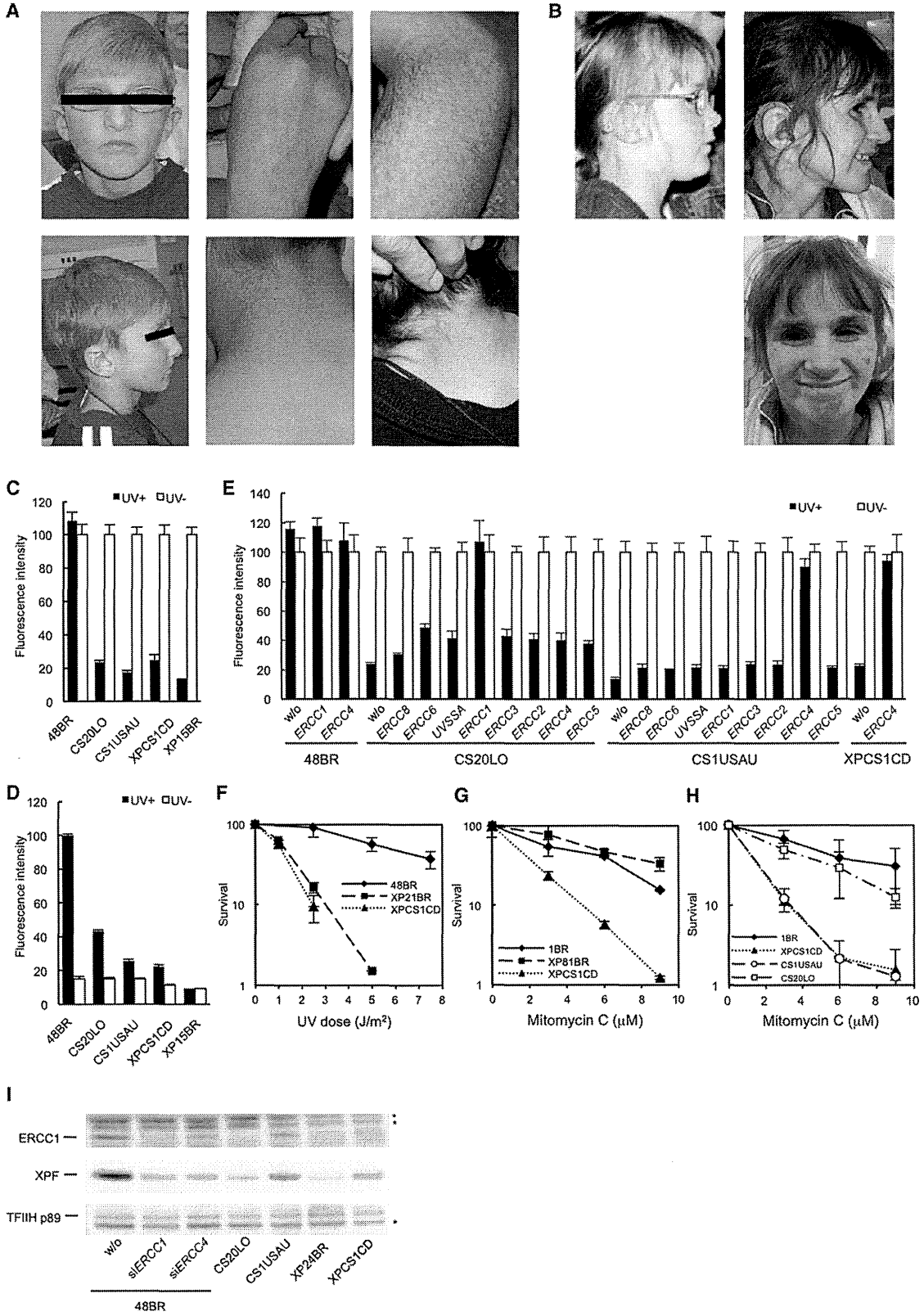

Figure 1. Three CS Individuals Belong to the ERCC1 and XP-F Complementation Groups

(A) CS1USAU, aged 8 years (left and middle panels) and 16 years (right panels). Note the pigmentation and hypopigmented maculas.

(B) XPCS1CD with features of XP, CS, and FA at 7.5 (left) and 11 years old (right).

(C) Reduction of RRS rates after UV irradiation in three CS cell lines (filled bars, 11 J/m^2 UVC; empty bars, no UV). RRS was measured by ethynyluridine (EU) incorporation and nuclear fluorescence detection (EU assay). 48BR is a normal control, CS20LO, CS1USAU, and XPCS1CD are CS cells, and XP15BR is affected by XP complementation group A (XP-A).

(D) Reduced level of unscheduled DNA synthesis (UDS) in the CS cells (filled bars, 20 J/m^2 UVC; empty bars, no UV).

(legend continued on next page)

(*CSA*) or *ERCC6* (*CSB*),[5] the products of which function, together with UVSSA (the product of the gene defective in UV-sensitive syndrome 3 [UVSS3 (MIM 614640), also known as UVSS-A])[6–8] in the still poorly understood initiation reaction of TC-NER, namely, the processing of the elongating form of RNA polymerase II stalled at the site of UV-induced DNA damage. These products thereby facilitate further recruitment of TFIIH, XPA, and NER incision endonucleases, ERCC1-XPF (ERCC4) and XPG (ERCC5), to carry out the removal of photolesions from actively transcribed genes.[4] In contrast to TC-NER, GG-NER is a genome-wide repair mechanism, and it shares the later steps with TC-NER and is deficient in several types of XP and XPCS.

The lack of TC-NER, as found in CS, can be assessed by a deficiency in the RRS test, which measures the *r*ecovery of *R*NA *s*ynthesis after UV irradiation. Another marker for DNA repair activity, the unscheduled DNA synthesis (UDS) test measures the GG-NER activity as the level of dNTP incorporation during DNA-repair synthesis after UV damage. Being negative for RRS and positive for UDS is diagnostic for CS. We have developed an efficient system for measuring RRS and UDS activities by using the incorporation of ethynyluracil derivatives and automated fluorescence-based imaging.[9,10] In a previous report, we sequenced all coding exons and their neighboring exon-intron boundaries of *ERCC8*, *ERCC6*, and *UVSSA* of 61 CS individuals whose genetic and/or molecular defects had not yet been determined so that we could evaluate whether *UVSSA* mutations might also result in CS phenotypes.[6] Although we did not identify any CS pathogenic mutation in *UVSSA*, we did identify several CS individuals who did not appear to have any causal mutations in *ERCC8*, *ERCC6*, or *UVSSA*, suggesting that additional gene(s) involved in TC-NER remain to be discovered.

Here, we report on three CS individuals who have normal *ERCC8* and *ERCC6* but have a defect in either *ERCC1* or *ERCC4* (*XPF*). In two cases, the affected individuals displayed typical CS clinical features (CS types I and II). In the third case, the affected individual not only had the combined XPCS phenotype but also had features of a third DNA-repair disorder, Fanconi anemia (FA [MIM 227650]). We propose that *ERCC1* and *ERCC4* be included as CS- and FA-associated genes.

CS20LO (photographs unavailable) was the daughter of nonconsanguineous parents and had an uneventful antenatal period. At 4–6 months of age, she had microcephaly, micrognathia, and contractures in the knees and elbows and was hypertonic with a dislocated radial head, deep-set eyes, and several moderate skeletal abnormalities, including camptodactyly, adducted thumbs, stiff limbs, steeply sloping acetabulae, wrist contracture, slender long bones with mildly flared metaphyses, and moderate kyphoscoliosis. She displayed brisk reflexes, and there were no feeding concerns. The karyotype was normal. Brain MRI at birth indicated a possible polymicrogyria; a nuclear-magnetic-resonance scan when she was 4 months old revealed large (>2 cm in depth) bilateral subdurals but no major visible malformations. An abnormal electroencephalogram was noticed at 9 months of age. At 16 months of age, she had nystagmus but no additional ophthalmic abnormalities; her corneas were completely clear and showed no evidence of cataracts. The diagnosis was confirmed as CS type II (early onset) because of RRS deficiency (see below). She died at the age of 2.5 years.

CS1USAU (Figure 1A) was born at around 41 weeks with a birth weight of 2.9 kg. He was prenatally diagnosed with microcephaly. His head circumference was at about the 9th percentile in the first few months and was lower than the 2nd percentile by 1 year of age. He developed normally for the first year without obvious abnormalities, except for the microcephaly. At the age of 5 years, he developed multiple unusual plantar warts on his hands and forearms. He had unusual freckling on his hands and the back of his neck and tended to burn easily and quickly, but did not blister badly, when he was exposed to sunlight. Since then, he has been well protected from solar exposure. At 7 years of age, he had deep-set eyes, progressive scoliosis, and multiple contractures in his feet; he required lengthening of the Achilles tendon because of muscle cramps in his hamstrings and calves. His skin was deeply pigmented with rashes and flat freckles. He displayed moderate bilateral hearing impairment, especially in the higher tones (he had normal hearing before the age of 3 years), short stature (height of 110.4 cm [<2nd percentile] and weight of 16.3 kg [<3rd percentile]), microcephaly (head circumference of 45.5 cm [<2nd percentile]), and circulatory problems. He had bilateral astigmatism but no cataracts,

(E) Complete rescue of the RRS deficiency by the infection of recombinant lentivirus expressing *ERCC1* cDNA in CS20LO cells and *ERCC4* cDNA in CS1USAU and XPCS1CD cells (filled bars, 10 J/m^2 UVC; empty bars, no UV).
(F) The colony-forming ability of XPCS1CD cells after UVC irradiation was compared with that of a normal control (48BR) and that of a cell strain with XP complementation group C (XP21BR).
(G) The colony-forming ability of XPCS1CD cells was compared with that of a normal control (1BR) and that of an XP-A cell strain (XP81BR) after treatment with different doses of mitomycin C (MMC) for 10 min.
(H) MMC sensitivity of different cell strains was determined by MMC treatment for 10 min and measurement of their viability by their ability to incorporate ^{3}H-thymidine (5 μCi/ml; 3 hr incubation) 3 days after treatment.
(I) Immunoblotting of ERCC1 and XPF in cells from CS individuals, *ERCC4*-deficient XP24BR cells, and normal 48BR cells with the TFIIH-p89 (XPB) subunit as a loading control. 48BR cells were mock transfected or transfected with siRNAs targeting either *ERCC1* or *ERCC4*. Asterisks indicate nonspecific bands. RRS was normalized to activity in nonirradiated cells. UDS activity was normalized to that of normal 48BR cells.
Error bars represent the SD of medians of nuclear fluorescence measurements in quintuplicate samples in (C)–(E) and the SD of means of triplicate experiments in (F)–(H).

attention deficit hyperactivity disorder, and learning disability. There were no obvious abnormalities apart from some delayed myelination on brain MRI at the age of 3 years, although basal ganglia T1 shortening was observed at the age of 7 years. He had severe migraines and headaches. His ambulation lessened over time, and he needed a gastrostomy-jejunostomy tube for feeding. Diagnosis of CS was confirmed at the age of 7 years because of RRS deficiency (see below). He is currently 16 years old.

XPCS1CD (Figure 1B) was the second child of nonconsanguineous parents. Intrauterine growth failure was noted during pregnancy, and therefore labor was induced at 38 weeks. Her birth weight was between the 0.4^{th} and 2^{nd} percentiles, her developmental milestones were globally delayed, and she required speech therapy. By 18 months of age, she was reported to sunburn with minimal sun exposure in both winter and summer months in the UK. Her parents described that sunburns would develop 24 hr after exposure, peak at 2–3 days, and resolve after 10–14 days. As a result, she was carefully photoprotected and did not have any further sunburn reactions after 4 years of age. When she was 5 years old, she developed progressive bilateral sensorineural deafness, and 2 years later, she presented with worsening ataxia, tremor, and weakness. She had short stature and significant microcephaly. At the age of 7.5 years (Figure 1B, left), her height was 1.4 cm below the 0.4^{th} percentile and her occipitofrontal head circumference (OFC) was 6.5 cm below the 0.4^{th} percentile. By the age of 6 years, she was thrombocytopenic and neutropenic, coinciding with treatment for recurrent infections. Her blood film showed irregularly shaped cells, and she gradually became pancytopenic with transfusion dependence by the age of 9 years. Renal impairment was detected at the age of 10 years, when she presented with hypertension, nephrotic range proteinuria, and rising serum creatinine. The karyotype was normal.

Upon examination at 11 years of age (Figure 1B, right), she was microcephalic with an OFC well below the 0.4^{th} percentile and had extremely short stature. She had deep-set eyes, a prominent nose, small teeth, and freckling over the nose and cheeks. There was marked palmar erythema, and extensive plane warts were seen on the arms. Her skin had an aged appearance, particularly over the dorsal hands. She had five café-au-lait macules. Her neurological examination highlighted a resting tremor, head titubation, and an ataxic gait. She demonstrated saccadic eye movements and an element of vertical nystagmus. There was subtle pyramidal tract weakness distally with extensor plantar reflexes. Sensation was intact. Ophthalmological examination revealed hypermetropia and bilateral blepharitis, but no other ocular abnormalities. MRI of the brain showed increased signal in the peritrigonal white-matter bilaterally. A renal biopsy and bone marrow aspirate were performed under general anesthesia (when she was 11 years old). The bone marrow showed a profoundly hypocellular sample in which all three lineages were present, blast percentage was <1%, and dysplasia was minimal. No clonal cytogenetic abnormalities were detected. A simultaneous full blood count showed a haemoglobin level of 9.4 g/dl (11.5–15.5 g/dl), a red blood cell count of 2.98×10^{12}/l ($3.40–5.20 \times 10^{12}$/l), and a mean corpuscular volume of 95.0 fl (80.0–98.0 fl). Studies of liver function were normal. The renal biopsy showed areas of focal segmental glomerular sclerosis and evident thickening of the capillary basement membrane. There was a background of interstitial fibrosis and tubular atrophy with glomerular shrinkage. She died at the age of 12 years after acute deterioration of her renal function. A postmortem examination was not done.

Many of her features were characteristic of CS,[11] although pancytopenia and renal failure are not usually associated with this disorder. The exaggerated and prolonged sunburn reactions together with progressive freckling at sun-exposed sites were suggestive of XP, whereas the pancytopenia, bone marrow findings, and recurrent infections are features often seen in FA.

To determine DNA-repair activities in the CS individuals' cells, we established dermal fibroblast cultures from skin biopsies. Written informed consent was obtained from the individuals' families, and the experiments were carried out in accordance with the local ethical standards (Nagasaki University Ethical, Legal, and Social Implications committee). We first measured the RRS rate after exposure to 10 J/m^2 UVC irradiation.[6,9,10] RNA-synthesis activity was significantly reduced in all three CS cell lines compared with normal cells (Figure 1C), indicating a deficiency in TC-NER activity, as expected for CS cells. We also measured UDS, a mark of GG-NER activity,[6,9,10] which is not normally affected in CS cells.[12] We found a significant reduction in UDS rates in all three CS cell lines (Figure 1D). These results imply that the CS individuals have defective GG-NER and TC-NER pathways, and we therefore presumed that, unlike other CS individuals, they carry defects in genes that commonly function in both the TC-NER and GG-NER pathways. Consequently, we anticipated that these three CS individuals might carry mutations either in *ERCC3* (*XPB*), *ERCC2* (*XPD*), *ERCC4*, or *ERCC5* (*XPG*) or in *ERCC1*, and we assayed complementation of the RRS defects by infecting the CS cells lines with recombinant lentiviruses expressing one of these NER-related cDNAs[6] (Figure 1E). The RRS defects were dramatically and specifically restored when CS20LO cells were infected with lentiviruses expressing *ERCC1* and when CS1USAU and XPCS1CD cells were infected with *ERCC4* cDNA, but not when the cells were infected with other viruses (Figure 1E). We conclude that CS20LO is assigned to the ERCC1 complementation group and that, likewise, CS1USAU and XPCS1CD are assigned to XP complementation group F (XP-F).

A hallmark of cells from individuals with FA is a specific defect in the repair of DNA interstrand crosslinks (ICLs). The ERCC1-XPF complex, which is uniquely among the NER proteins, is also involved in ICL repair.[13,14] Because several clinical features of XPCS1CD are characteristic of

FA, we measured the survival of this individual's cells after exposure to UV irradiation and to the crosslinking agent mitomycin C (MMC). Figure 1F shows that cells from XPCS1CD are as sensitive to UV irradiation as those from an XP control. In contrast, the XP control cells (in this case, from group A) are, as reported in the literature,[15] not sensitive to MMC, whereas XPCS1CD cells are much more sensitive (Figure 1G). Furthermore, chromosome-breakage studies on blood showed increased sensitivity to MMC and an elevated level of chromosome damage upon exposure to the alkylating agent DEB (1,2,3,4-diepoxybutane). However, the levels were lower than expected for a diagnosis of FA (data not shown). In view of these observations, we also examined the MMC sensitivity of CS1USAU and CS20LO cells and found that the former were also very sensitive to MMC, whereas the latter were marginally, if at all, sensitive (Figure 1H).

ERCC1 is needed for stabilizing and enhancing XPF endonuclease activity,[16,17] and indeed, using immunoblotting, we observed a significant reduction in the expression level of XPF concurrently with the reduction of ERCC1 expression in CS20LO cells (Figure 1I). In contrast, XPF and ERCC1 levels were modestly reduced in CS1USAU and XPCS1CD cells (Figure 1I).

To determine the genetic changes in the three CS individuals, we carried out (1) PCR-based gDNA amplification of the exons and neighboring exon-intron boundaries of *ERCC1* from CS20LO cells and of *ERCC4* from CS1USAU cells and subsequent direct sequencing of the amplified gDNA fragments and (2) RT-PCR of mRNA and sequencing of the cDNA from XPCS1CD cells. In CS20LO cells, a homozygous mutation, c.693C>G, in exon 7 of *ERCC1* (RefSeq accession number NM_001983.3) resulted in amino acid substitution p.Phe231Leu, located in the C-terminal XPF-interacting helix-hairpin-helix (HhH) domain (Figure 2A). ERCC1 pathogenic changes identified in NER-deficient diseases and in other genetic disorders are extremely rare; only two cases have been reported.[18,21] Individual 165TOR,[21] who had clinical features overlapping those of CS and was diagnosed with a severe form of COFS, was heterozygous for the *ERCC1* c.693C>G (p.Phe231Leu) mutation found in our CS individual. In 165TOR, the other *ERCC1* pathogenic allele was c.472C>T (p.Gln158*); however, the mutated transcript is presumed to be subject to nonsense-mediated mRNA decay (NMD). XP202DC[18] was a XP individual who developed progressive neurodegeneration during adolescence and died at the age of 37 years. He was compound heterozygous for nonsense substitution p.Lys226* near the C terminus and splice-site mutation c.604-26G>A, which might have affected the expression level of wild-type ERCC1. In this individual, a low amount of the wild-type *ERCC1* allele expression might have been sufficient to ameliorate the more severe aspects of the disorder.

CS1USAU cells had two heterozygous mutational changes in *ERCC4* (RefSeq NM_005236.2): (1) an exon 4 mutation, c.706T>C, causing an amino acid substitution, p.Cys236Arg, located in the N-terminal large SF2 helicase domain and (2) an exon 8 frameshift insertion, c.1730_1731insA, which generated a premature stop codon, p.Tyr577* (Figure 2B). XPCS1CD had two *ERCC4* heterozygous mutations, c.706T>C and c.1765C>T, resulting in changes p.Cys236Arg (the same mutation as we found in CS1USAU) and p.Arg589Trp (previously found in three XP individuals) (Figure 2C), respectively.[18] Previously identified alterations in ERCC1 and XPF, together with those identified in this paper, are shown in Figure 2D.

XPF pathogenic alterations are normally associated with mild XP cases without severe developmental abnormalities.[18] There has been one exceptional case, XFE progeroid syndrome (MIM 610965). The affected individual, XP51RO, carried a homozygous mutation resulting in a p.Arg153Pro change in the SF2 domain of XPF.[22] In all reported cases with mild XP-F, the pathogenic mutations are hypomorphic and there is a substantial amount of residual XPF in the cells; however, in the XFE individual cells, XPF expression was severely reduced.[22] In contrast, in CS1USAU and XPCS1CD cells, a substantial amount of XPF remained (Figure 1I), suggesting that the pathogenic allele is fully expressed and the altered protein is stable (also see later purification of the ERCC1-XPF complex). These observations indicate that p.Cys236Arg causes XPF dysfunction and confers a CS phenotype on individuals CS1USAU and XPCS1CD.

XPF and ERCC1 form a heterodimeric structure-specific endonuclease, the ERCC1-XPF complex, which cleaves on the 5′ side of the UV-damaged DNA at the incision step of NER.[23–25] The proteins form a complex through their C-terminal HhH domains and stabilize the counterpart when in a complex. To test whether the p.Phe231Leu altered ERCC1 and the p.Cys236Arg altered XPF form proper ERCC1-XPF complexes, we introduced the altered proteins (V5-tagged) into 293FT cells and performed immunoprecipitation to check the binding affinity between ERCC1 and XPF. Although the ERCC1 p.Phe231Leu substitution is located in the XPF-binding HhH domain and the residue interfaces with two alpha helices of the XPF HhH domain, the altered ERCC1 binding capacity to XPF was unaffected by the substitution (Figure 3A). Similarly, we observed no significant decrease in coprecipitation of wild-type ERCC1 in the complex when p.Cys236Arg XPF was expressed (Figure 3B). The ERCC1-XPF complex also interacts with TFIIH, as shown by both in vitro and in vivo experiments.[26] We therefore tested the binding affinity of altered ERCC1 and XPF with the XPB-p89 subunit of TFIIH. Although there was no significant reduction in binding affinity of p.Phe231Leu ERCC1 expressed in 293FT cells (Figure 3A), we observed, after UV irradiation, less p89 in immunoprecipitates from cells expressing p.Cys236Arg XPF than from wild-type controls (Figure 3B). Recent studies also demonstrated that the three known structure-specific endonuclease complexes (SSEs)—ERCC1-XPF, SLX4 (FANCP)-SLX1, and MUS81 (SLX3)-EME1 (SLX2)—interact with each other in

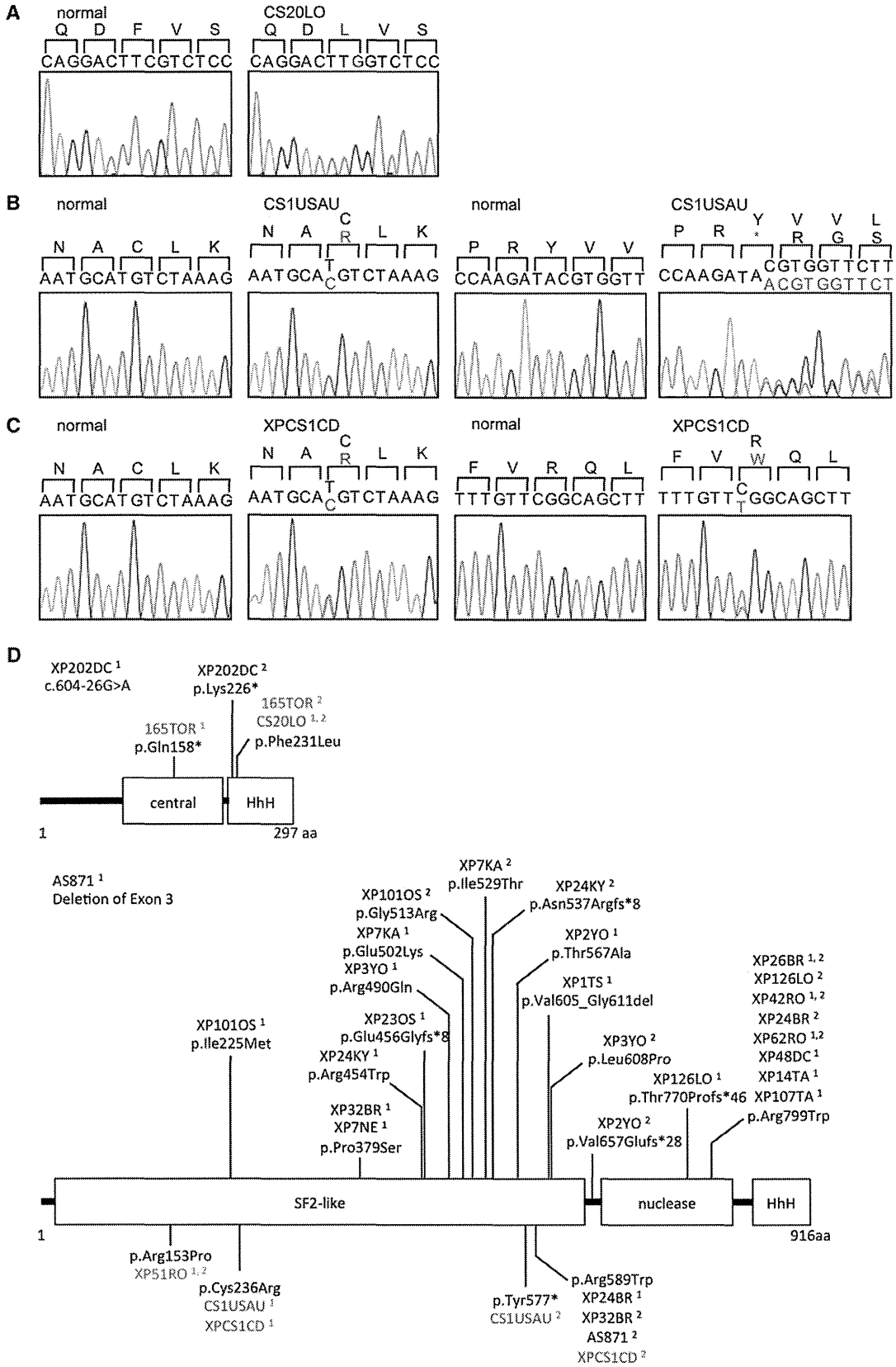

Figure 2. Locations of the *ERCC1* and *ERCC4* Mutations Identified in the CS Cells and in Known NER Disorders
(A) The homozygous c.693C>G single-nucleotide variant (SNV) in *ERCC1* exon 7 in the CS individual, CS20LO; the altered amino acid, Phe231, is shown in red.
(B) The heterozygous c.706T>C SNV in *ERCC4* exon 4 and the 1 base insertion, c.1730_1731insA, in *ERCC4* exon 8 are identified in the CS individual, CS1USAU. The altered amino acids, Cys236 and Tyr577, are shown in red.

(legend continued on next page)

crosslink-repair pathways. Importantly, mutations in *SLX4* have been identified in several FA individuals, and SLX4 acts as a scaffold and plays a key role in the coordination of these interactions.[27–29] We therefore tested whether one of these interactions, namely the binding affinity of the altered protein with MUS81 (Figure 3B), is compromised in cells expressing the XPF p.Cys236Arg substitution. There was no impact on the binding affinity, suggesting that this was not the cause of the FA features observed in XPCS1CD.

To further test whether the altered ERCC1 and XPF proteins retain any DNA-repair functions, we performed complementation analyses of the RRS defects by expressing mutant *ERCC1* and *ERCC4* cDNAs in the ERCC1- and XPF-deficient CS cells, respectively (Figure 3C). Consistent with the previous report describing a correction of UV sensitivity after transfection with the *ERCC1* c.693C>G (p.Phe231Leu) pathogenic mutant cDNA into ERCC1-deficient 165TOR cells,[21] we observed that RRS in the ERCC1-deficient CS20LO cells was fully restored upon infection with the lentivirus expressing c.693C>G (p.Phe231Leu) mutant *ERCC1* cDNA, whereas expression of the p.Cys236Arg altered XPF failed to restore RRS levels of the XPF-deficient CS1USAU cells.

We then purified recombinant ERCC1-XPF complexes and determined their endonuclease activity. As observed in Figure 1I, the altered p.Cys236Arg XPF complex was stable (Figure 3D). Because stem-loop structures are good substrates for the ERCC1-XPF complex,[30] we performed in vitro incision assays with fluorescent-labeled DNA templates containing a 12 bp stem-dT22-loop.[19,30] We observed significant reduction of the endonuclease activity of the p.Cys236Arg altered complex (Figure 3E).

These data indicate that XPF malfunction, caused by the lack of proper interaction between TFIIH and ERCC1-XPF, and a substantial reduction of the stem-loop incision activity of the endonuclease complex cause the CS and FA phenotypes in CS1USAU and XPCS1CD, whereas the reason for ERCC1 deficiency in CS20LO cells remains unclear.

Unlike NER-associated genes that are responsible exclusively for CS and UVSS phenotypes (i.e., *ERCC8*, *ERCC6*, and *UVSSA*), *ERCC4* and *ERCC1* are presumably indispensable for fetal development because there is no known individual carrying homozygous or compound-heterozygous null mutations in either of the genes. Given that we found that the p.Phe231Leu altered ERCC1 retains normal NER function, we decided to determine the precise expression levels of the mutant *ERCC1* and *ERCC4* alleles identified in two of the CS individuals. We undertook allele-specific quantitative RT-PCR (qRT-PCR) with sets of primers that selectively amplify the wild-type or the mutant *ERCC1* and *ERCC4* cDNAs (Table 1). In CS20LO cells, primer set ERCC1-WT and ERCC1-Rv1 allowed specific amplification of the wild-type *ERCC1* allele (Figure 4A, left), whereas another set of primers, ERCC1-p.Phe231Leu and ERCC1-Rv1, amplified the c.693C>G (p.Phe231Leu) allele in exon 7 (Figure 4A, middle); primers ERCC1-com1 and ERCC1-Rv1 amplified both the wild-type and the mutant alleles (Figure 4A, right). We observed a very low level (50-fold < wild-type) of expression of the *ERCC1* c.693C>G (p.Phe231Leu) allele in CS20LO cells (Figure 4A, middle and right), suggesting that the ERCC1-null phenotype can be ascribed to this drastic attenuation of *ERCC1* mRNA expression. Subsequently, expression of the wild-type and the two mutated *ERCC4* alleles in CS1USAU cells was examined. Similarly to how we quantified *ERCC1* mRNA, we designed sets of primers to specifically amplify the c.706T>C (p.Cys236Arg) allele located in exon 4 (Figure 4B, middle) and the c.1730_1731insA (p.Tyr577*) allele in exon 8 (Figure 4C, middle), as well as their corresponding wild-type alleles (Figure 4B and 4C, left). We confirmed the expression of the c.706T>C (p.Cys236Arg) allele specifically in CS1USAU cells (Figure 4B, middle and right) with primers XPF-p.Cys236Arg and XPF-Rv1, whereas the c.1730_1731insA (p.Tyr577*) allele, measured by primers XPF-p.Tyr577* and XPF-Rv2, was subjected to NMD, because its expression level was very low in the CS cells (Figure 4C, middle). Given these qRT-PCR data and the protein expression levels in the CS cells (Figure 1I), we conclude that the ERCC1-deficiency phenotype in CS20LO results from a very low level of expression of the mutant allele and that the XPF deficiency in CS1USAU and XPCS1CD is mainly caused by protein malfunction. A summary of our findings is presented in Table 2.

We have identified three CS individuals who carry pathogenic mutations in either *ERCC1* or *ERCC4*. Approximately 25 XP-F individuals have been described in the literature.[18] The majority of them are XP individuals, who, compared with individuals affected by XP complementation group C, have relatively mild skin problems and skin cancers that appear relatively later in life. Only XFE individual XP51RO had a much more severe phenotype.[22] Like our CS individuals, he had short stature, cachexia, and microcephaly. He had mild learning difficulties, hearing loss, and visual impairment. He was sensitive to the sun from birth and had dry, atrophic skin and irregular pigmentation on sun-exposed areas. Laboratory studies indicated renal insufficiency, and he died at the age of 16 years from severe pneumonia and multisystem organ failure. This individual had many features in common with XPCS1CD, but there was no report of pancytopenia. He was homozygous for p.Arg153Pro in XPF.

(C) The heterozygous c.706T>C SNV in *ERCC4* exon 4 and the heterozygous c.1765C>T SNV in XPCS1CD. The altered amino acids, Cys236 and Arg589, are shown in red.
(D) The structure of ERCC1 and XPF and the amino acid alterations reported here and published previously.[18–20] The cases shown in colors are as follows: XP, black; COFS, blue; XFE, green; and CS or XPCS, red. Superscripted 1 and 2 designate the number of discrete alleles.

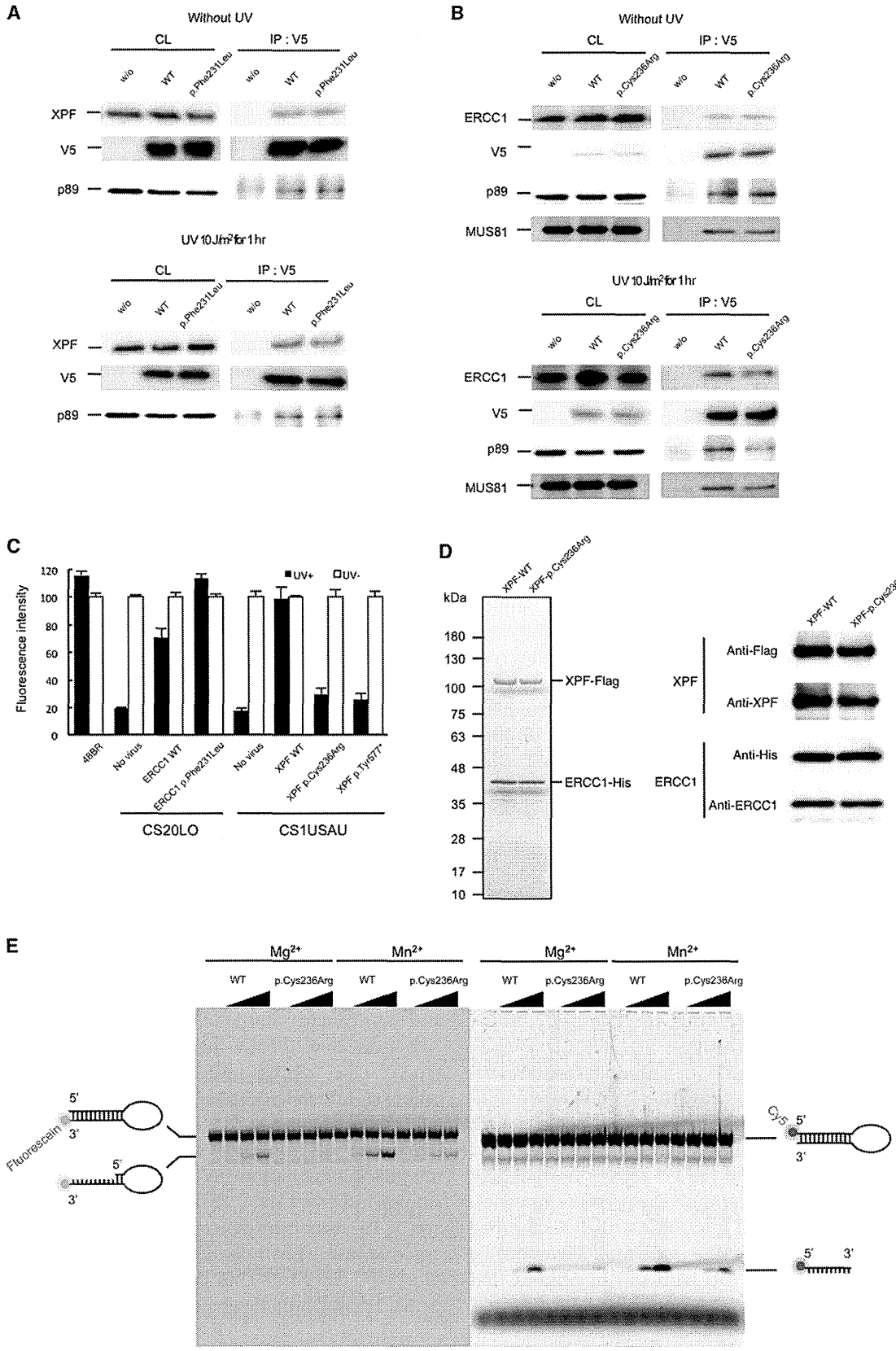

Figure 3. ERCC1 and XPF Interaction in the CS Cells

(A) V5-tagged wild-type and p.Phe231Leu altered ERCC1 interactions with the endogenous wild-type XPF were assayed by immunoprecipitation either without UV irradiation or 1 hr after 10 J/m^2 of UV irradiation.

(B) V5-tagged wild-type and p.Cys236Arg altered XPF were expressed in 293T cells, and interactions with the endogenous wild-type ERCC1 were assayed by immunoprecipitation from extracts of cells either without UV irradiation or 1 hr after 10 J/m^2 of UV irradiation.

(legend continued on next page)

Table 1. Primers Used for Allele-Specific Amplifications

Primer Designation	Primer Sequence
ERCC1-WT1	5′- CTGATGGAGAAGCTAGAGCAGGACTTC-3′
ERCC1-p.Phe231Leu	5′- CTGATGGAGAAGCTAGAGCAGGACTTG-3′
ERCC1-com1	5′- CCTGATGGAGAAGCTAGAGCAGGACTT-3′
ERCC1-Rv1	5′- GGTCAGACATTCAGTCACCCGC-3′
XPF-WT1	5′- GACTGCTATACTGGACATTTTAAATGCAT-3′
XPF-p.Cys236Arg	5′- GACTGCTATACTGGACATTTTAAATGCAC-3′
XPF-com1	5′- AGACTGCTATACTGGACATTTTAAATGCA-3′
XPF-Rv1	5′- TCCAAGCTGGTGCCACAAA-3′
XPF-WT2	5′- AGGGTACTACATGAAGTGGAGCCAAGAT AC-3′
XPF-p.Tyr577*	5′- AGGGTACTACATGAAGTGGAGCCAAGAT AA-3′
XPF-com2	5′- AAGGGTACTACATGAAGTGGAGCCAAGA TA-3′
XPF-Rv2	5′- CCCTCAGAGGTTTCCCAGGC-3′

Somewhat surprisingly, the previously reported *ERCC1*-deficient severe COFS individual was compound heterozygous for the same pathogenic p.Phe231Leu change together with a termination substitution, p.Gln158*,[21] whereas our CS type II individual was homozygous for this substitution. Because the p.Phe231Leu altered ERCC1 retained normal function, differences in severity of the clinical features might be explained by the dosage of *ERCC1* expression. We hypothesize that the relatively milder clinical features observed in our CS individual might be due to the fact that the biallelic expression of the mutated *ERCC1* allele produced twice the level of functional ERCC1 in the CS individual as in the COFS individual. This idea is also supported by the observation that the other *ERCC1*-deficient XP individual, who displayed milder clinical features, harbored a splice-site mutation that most likely allowed readthrough of a significant amount of normal protein.

We identified a heterozygous XPF alteration, p.Cys236Arg, in CS individuals CS1USAU and XPCS1CD. CS1USAU displayed mild skin problems in the range defined by normal CS features, but he has been very well protected from sun exposure. He displayed hypopigmented macules (Figure 1A), which are typical of XP and often occur on the limbs and other sun-exposed sites before "freckling." In view of this and his early freckling, it seems appropriate to classify this affected individual as also having the combined XPCS phenotype. However, XPCS1CD, but not CS1USAU, also exhibited hematological abnormalities characteristic of FA. Surprisingly, the second allele in the milder individual, CS1USAU, was a functionally null termination mutation, which was subjected to NMD, whereas in the more severely affected XPCS1CD, the second allele harbored c.1765C>T (p.Arg589Trp), which is found in several XP individuals and results in mislocalization of the ERCC1-XPF complex to the cytoplasm and thus causes a severe XP phenotype when combined with certain other alleles.[19] XP32BR (with p.Arg589Trp and p.Pro379Ser) was a mildly affected XP individual in his teens and had no neurological problems; XP24BR (with p.Arg589Trp and p.Arg799Trp) was also mildly affected but is now showing some abnormal neurological and CS-like facial features in her 40s (our unpublished data); AS871 (with p.Arg589Trp resulting from

Interactions were detected by immunoblotting with antibodies against the V5-tagged ERCC1 and XPF (1H6, MBL), MUS81 (MTA30 2G10/3, Santa Cruz), ERCC1 (8F1, Santa Cruz), and XPF (Ab-1, Thermo scientific). Abbreviations are as follows: CL, crude lysate (10% load); and IP, immunoprecipitate.

(C) Rescue of the RRS deficiency was assayed by the infection of recombinant lentivirus expressing either wild-type or mutant *ERCC1* and *ERCC4* cDNAs (filled bars, 11 J/m^2 UV; empty bars, no UV). RRS was normalized to activity in nonirradiated cells. Error bars represent the SD of medians of nuclear fluorescence measurements in quintuplicate samples.

(D) Purification of the recombinant ERCC1-XPF complexes. FLAG-tagged (C terminus) wild-type and p.Cys236Arg altered XPF were coexpressed with the 6 × His-tagged ERCC1 (C terminus) in 293T cells. The cells were harvested and lysed in lysis buffer (50 mM Tris-HCl, 150 mM KCl, 1 mM EDTA, 1% NP-40, 10% glycerol, 0.25 mM PMSF, protease-inhibitor cocktail [PIC, Roche], pH 7.5). Tandem affinity purification was performed with mouse anti-FLAG IgG-conjugated beads (M2 agarose, SIGMA) followed by TALON metal affinity resin (Clontech). Cell lysates were incubated with anti-FLAG agarose beads and were subsequently washing with salt buffer (20 mM Tris-HCl, 1 M KCl, 0.1 mM EDTA, 10% glycerol, PIC, pH 7.5) and starting buffer (20 mM Tris-HCl, 800 mM KCl, 10% glycerol, 10 mM imidazole, PIC, pH 7.5). Binding proteins were eluted with starting buffer containing 1 mg/ml FLAG peptide. The eluted fractions were incubated with TALON metal affinity resin (Clontech) and were then sequentially washed with buffer A (40 mM HEPES, 1,000 mM NaCl, 10% glycerol, 10 mM Imidazole, PIC, pH 7.5) and buffer B (40 mM HEPES, 100 mM NaCl, 10% glycerol, 10 mM Imidazole, PIC, pH 7.5). The purified complex was sequentially eluted with elution buffer A (40 mM HEPES, 100 mM NaCl, 10% glycerol, 100 mM Imidazole, PIC, pH 7.5) and elution buffer B (40 mM HEPES, 100 mM NaCl, 10% glycerol, 300 mM Imidazole, pH 7.5). Purified complex was dialyzed against GF buffer (25 mM HEPES, 150 mM NaCl, 10% glycerol, 5 mM beta-mercaptoethanol, PIC, pH 8.0) and concentrated. The purified complexes were resolved by SDS-PAGE and detected by silver staining (100 ng of total protein). Purity of the complexes was assessed by immunoblotting with antibodies against the FLAG (MBL) and 6 × His (MBL) tags, as well as ERCC1 and XPF. No endogenous XPF was detected.

(E) Endonuclease activity of the wild-type and altered ERCC1-XPF complexes was determined with fluorescently labeled 12 bp stem-dT22-loop DNA templates. Either 3′-fluorescein- or 5′-Cy5-labeled oligonucleotides (5′-GCCAGCGCTCGG-dT22-CCGAGCGCTGGC-3′) were purchased from SIGMA and self-annealed in TE buffer. Nuclease incision reactions were performed on 200 fmol of the DNA templates and 0, 25, 50, 100 ng of the purified ERCC1-XPF complexes in a total volume of 15 μl nuclease reaction buffer (25 mM HEPES, 40 mM NaCl, 10% glycerol, 0.5 mM beta-mercaptoethanol, and 0.1 mg/ml BSA and either 2 mM $MgCl_2$ or 0.4 mM $MnSO_4$, pH 8.0). The reaction mixtures were incubated at 30°C for 1 hr. Samples were separated on urea-denatured 15% PAGE, and the cleaved products were analyzed by a Typhoon imager (GE).

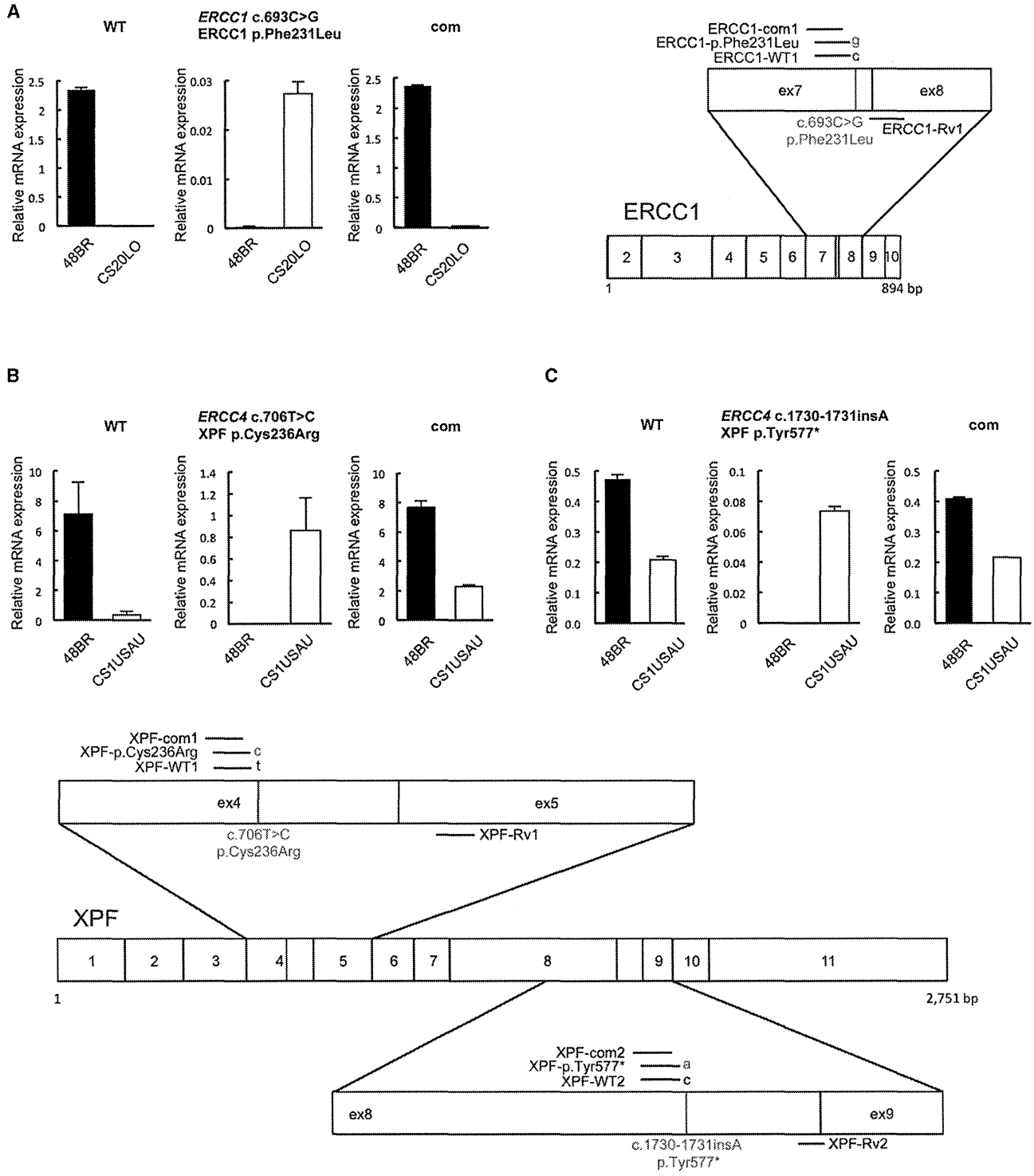

Figure 4. Expression of the Pathogenic Alleles in the CS Cells

Total RNA was extracted with ISOGEN reagent (NIPPON GENE) according to the manufacturer's instruction. One microgram of total RNA was reverse transcribed with a high-capacity RNA-to-cDNA kit (Applied Biosystems, Life Technologies). Quantitative PCR amplification and real-time detection were carried out in a Thermal Cycler Dice Real-Time System (TaKaRa Bio) with SYBR Premix Ex TaqII (TaKaRa Bio) and a QuantiTect SYBR Green PCR kit (QIAGEN). For each sample, relative mRNA levels were normalized against *HPRT1* mRNA expression. Error bars represent the SD of means of triplicate experiments.

(A) Selective quantitative amplification of the wild-type and the mutated c.693C>G (p.Phe231Leu) *ERCC1* alleles in CS20LO cells and normal 48BR cells. Allele-specific primers selectively amplified the wild-type (c.693C) allele (ERCC1-WT1 and ERCC1-Rv1, left panel), the CS pathogenic mutant (c.693C>G) allele (ERCC1-p.Phe231Leu and ERCC1-Rv1, middle panel), and both alleles at once (ERCC1-com1 and ERCC1-Rv1, right panel).

(B) Selective quantitative amplification of the wild-type and the mutated c.706T>C (p.Cys236Arg) *ERCC4* alleles in CS1USAU cells and normal 48BR cells. Allele-specific primers selectively amplified the wild-type (c.706T) allele (XPF-WT1 and XPF-Rv1, left panel), the CS

(legend continued on next page)

Table 2. Summary of Phenotypes of CS Cells

	Individual		
	CS20LO	**CS1USAU**	**XPCS1CD**
RRS	–	–	–
UDS	–	–	–
Virus complementation with *ERCC1* wild-type cDNA (RRS)[a]	+	–	–
Virus complementation with *ERCC4* wild-type cDNA (RRS)[a]	–	+	+
XPF expression	–	+/–	+/–
ERCC1 expression	–	+/–	+/–
Protein alteration	ERCC1 p.Phe231Leu	XPF p.Cys236Arg and p.Tyr577*	XPF p.Cys236Arg and p.Arg589Trp
ERCC1-XPF IP	+	+	+ (p.Cys236Arg)
p89 IP	+	+/–	+/– (p.Cys236Arg)
Virus complementation with *ERCC1* c.693C>G (p.Phe231Leu) cDNA (RRS)[a]	+	ND	ND
Virus complementation with *ERCC4* c.706T>C (p.Cys236Arg) cDNA (RRS)[a]	ND	–	ND
ERCC1-XPF nuclease activity	ND	– (p.Cys236Arg)	– (p.Cys236Arg)
Mutant mRNA level	V low	+/–	ND

Abbreviations are as follows: +, normal; –, defective or absent; +/–, intermediate; IP, immunoprecipitation; ND, not done.
[a]Effect of the indicated cDNA on the RRS response.

the deletion of exon 3) had severe skin symptoms and neurodegeneration.[19] The reason why a partially functional allele (c.1765C>T [p.Arg589Trp]) in XPCS1CD results in a more severe phenotype than the null allele in CS1USAU is currently unclear.

Mice homozygous for a frameshift mutation in *Ercc4* (*Xpf*) die by 3 weeks of age.[31] Likewise, mice in which *Ercc1* has been deleted die soon after birth.[32,33] They develop progressive neurodegeneration, leucopenia and thrombocytopenia,[22] and impaired liver function.[32] Many of these characteristics resemble those of XPCS1CD. Pancytopenia is a hallmark of FA, a disorder associated with cellular hypersensitivity to DNA-ICL-inducing agents.[34] Recent data have indicated that endogenous aldehydes generate DNA damage that requires the FA pathway for resolution.[35] We therefore favor the explanation that pancytopenia arises from a defect in the response to such crosslinkers; this defect is common to the FA individuals and XPCS1CD (Figure 1G). Support for this idea comes from Bogliolo et al.,[36] who report on two FA individuals with mutations in *ERCC4* but without features of CS or XP.

Finally, our results demonstrate that *ERCC4* and *ERCC1* must be added to the list of genes in which defects can result in either CS or the combined XP-CS-FA phenotype.

Acknowledgments

This work was supported by KAKENHI Grants-in-Aid for Young Scientists A (24681008), Exploratory Research (24659533) from the Japan Society for the Promotion of Science, a science research grant from Inamori Foundation, a medical research grant from Mochida Memorial Founds for Medical and Pharmaceutical Research, a medical research grant from the Daiichi-Sankyo Foundation of Life Science, a grant for basic science research from The Sumitomo Foundation, and a medical research grant from Takeda Science Foundation to T.O.; Special Coordination Funds for Promoting Science and Technology from the Japan Science and Technology Agency to Y.N.; and a grant from the Associazione Italiana per la Ricerca sul Cancro (AIRC) to M.S. We are grateful to the National Commissioning Group of the UK National Health Service (NHS) for funding the xeroderma pigmentosum service. In addition, the authors acknowledge financial support from the UK Department of Health via the National Institute for Health Research comprehensive Biomedical Research Centre award to Guy's & St. Thomas' NHS Foundation Trust in partnership with King's College London and King's College Hospital NHS Foundation Trust. Some early experiments were carried out by Di J. Sun.

pathogenic mutant (c.706T>C) allele (XPF-p.Cys236Arg and XPF-Rv1, middle panel), and both alleles at once (XPF-com1 and XPF-Rv1, right panel).
(C) Selective quantitative amplification of the wild-type and the c.1730_1731insA (p.Tyr577*) *ERCC4* alleles. Allele-specific primers selectively amplified the wild-type (c.1731C) allele (XPF-WT2 and XPF-Rv2, left panel), the CS pathogenic mutant (c.1730_1731insA) allele (XPF-p.Tyr577* and XPF-Rv2, middle panel), and both alleles at once (XPF-com2 and XPF-Rv2). Locations of the primer sets used for the qRT-PCR experiments are depicted on the right-hand side. Transcripts from *HPRT1* were used as a quantification control. Primers used for the qPCR are listed in Table 1.

We are grateful to the families of the affected individuals for their helpful cooperation with these studies.

Received: November 20, 2012
Revised: March 14, 2013
Accepted: April 9, 2013
Published: April 25, 2013

Web Resources

The URLs for data presented herein are as follows:

GeneReviews, Laugel, V. (1993). Cockayne Syndrome, http://www.ncbi.nlm.nih.gov/books/NBK1342/
RefSeq, http://www.ncbi.nlm.nih.gov/RefSeq

References

1. Kleijer, W.J., Laugel, V., Berneburg, M., Nardo, T., Fawcett, H., Gratchev, A., Jaspers, N.G., Sarasin, A., Stefanini, M., and Lehmann, A.R. (2008). Incidence of DNA repair deficiency disorders in western Europe: Xeroderma pigmentosum, Cockayne syndrome and trichothiodystrophy. DNA Repair (Amst.) *7*, 744–750.
2. Laugel, V., Dalloz, C., Tobias, E.S., Tolmie, J.L., Martin-Coignard, D., Drouin-Garraud, V., Valayannopoulos, V., Sarasin, A., and Dollfus, H. (2008). Cerebro-oculo-facio-skeletal syndrome: three additional cases with CSB mutations, new diagnostic criteria and an approach to investigation. J. Med. Genet. *45*, 564–571.
3. Friedberg, E.C., Walker, G.C., Siede, W., Wood, R.D., Schultz, R.A., and Ellenberger, T. (2006). DNA Repair and Mutagenesis, Second Edition (Washington, DC: ASM Press).
4. Hanawalt, P.C., and Spivak, G. (2008). Transcription-coupled DNA repair: two decades of progress and surprises. Nat. Rev. Mol. Cell Biol. *9*, 958–970.
5. Laugel, V., Dalloz, C., Durand, M., Sauvanaud, F., Kristensen, U., Vincent, M.C., Pasquier, L., Odent, S., Cormier-Daire, V., Gener, B., et al. (2010). Mutation update for the CSB/ERCC6 and CSA/ERCC8 genes involved in Cockayne syndrome. Hum. Mutat. *31*, 113–126.
6. Nakazawa, Y., Sasaki, K., Mitsutake, N., Matsuse, M., Shimada, M., Nardo, T., Takahashi, Y., Ohyama, K., Ito, K., Mishima, H., et al. (2012). Mutations in UVSSA cause UV-sensitive syndrome and impair RNA polymerase IIo processing in transcription-coupled nucleotide-excision repair. Nat. Genet. *44*, 586–592.
7. Zhang, X., Horibata, K., Saijo, M., Ishigami, C., Ukai, A., Kanno, S., Tahara, H., Neilan, E.G., Honma, M., Nohmi, T., et al. (2012). Mutations in UVSSA cause UV-sensitive syndrome and destabilize ERCC6 in transcription-coupled DNA repair. Nat. Genet. *44*, 593–597.
8. Schwertman, P., Lagarou, A., Dekkers, D.H., Raams, A., van der Hoek, A.C., Laffeber, C., Hoeijmakers, J.H., Demmers, J.A., Fousteri, M., Vermeulen, W., and Marteijn, J.A. (2012). UV-sensitive syndrome protein UVSSA recruits USP7 to regulate transcription-coupled repair. Nat. Genet. *44*, 598–602.
9. Limsirichaikul, S., Niimi, A., Fawcett, H., Lehmann, A., Yamashita, S., and Ogi, T. (2009). A rapid non-radioactive technique for measurement of repair synthesis in primary human fibroblasts by incorporation of ethynyl deoxyuridine (EdU). Nucleic Acids Res. *37*, e31.
10. Nakazawa, Y., Yamashita, S., Lehmann, A.R., and Ogi, T. (2010). A semi-automated non-radioactive system for measuring recovery of RNA synthesis and unscheduled DNA synthesis using ethynyluracil derivatives. DNA Repair (Amst.) *9*, 506–516.
11. Nance, M.A., and Berry, S.A. (1992). Cockayne syndrome: review of 140 cases. Am. J. Med. Genet. *42*, 68–84.
12. Lehmann, A.R. (2003). DNA repair-deficient diseases, xeroderma pigmentosum, Cockayne syndrome and trichothiodystrophy. Biochimie *85*, 1101–1111.
13. Hoy, C.A., Thompson, L.H., Mooney, C.L., and Salazar, E.P. (1985). Defective DNA cross-link removal in Chinese hamster cell mutants hypersensitive to bifunctional alkylating agents. Cancer Res. *45*, 1737–1743.
14. Wood, R.D. (2010). Mammalian nucleotide excision repair proteins and interstrand crosslink repair. Environ. Mol. Mutagen. *51*, 520–526.
15. Fujiwara, Y. (1982). Defective repair of mitomycin C crosslinks in Fanconi's anemia and loss in confluent normal human and xeroderma pigmentosum cells. Biochim. Biophys. Acta *699*, 217–225.
16. van Vuuren, A.J., Appeldoorn, E., Odijk, H., Yasui, A., Jaspers, N.G., Bootsma, D., and Hoeijmakers, J.H. (1993). Evidence for a repair enzyme complex involving ERCC1 and complementing activities of ERCC4, ERCC11 and xeroderma pigmentosum group F. EMBO J. *12*, 3693–3701.
17. Biggerstaff, M., Szymkowski, D.E., and Wood, R.D. (1993). Co-correction of the ERCC1, ERCC4 and xeroderma pigmentosum group F DNA repair defects in vitro. EMBO J. *12*, 3685–3692.
18. Gregg, S.Q., Robinson, A.R., and Niedernhofer, L.J. (2011). Physiological consequences of defects in ERCC1-XPF DNA repair endonuclease. DNA Repair (Amst.) *10*, 781–791.
19. Ahmad, A., Enzlin, J.H., Bhagwat, N.R., Wijgers, N., Raams, A., Appledoorn, E., Theil, A.F., J Hoeijmakers, J.H., Vermeulen, W., J Jaspers, N.G., et al. (2010). Mislocalization of XPF-ERCC1 nuclease contributes to reduced DNA repair in XP-F patients. PLoS Genet. *6*, e1000871.
20. Matsumura, Y., Nishigori, C., Yagi, T., Imamura, S., and Takebe, H. (1998). Characterization of molecular defects in xeroderma pigmentosum group F in relation to its clinically mild symptoms. Hum. Mol. Genet. *7*, 969–974.
21. Jaspers, N.G., Raams, A., Silengo, M.C., Wijgers, N., Niedernhofer, L.J., Robinson, A.R., Giglia-Mari, G., Hoogstraten, D., Kleijer, W.J., Hoeijmakers, J.H., and Vermeulen, W. (2007). First reported patient with human ERCC1 deficiency has cerebro-oculo-facio-skeletal syndrome with a mild defect in nucleotide excision repair and severe developmental failure. Am. J. Hum. Genet. *80*, 457–466.
22. Niedernhofer, L.J., Garinis, G.A., Raams, A., Lalai, A.S., Robinson, A.R., Appeldoorn, E., Odijk, H., Oostendorp, R., Ahmad, A., van Leeuwen, W., et al. (2006). A new progeroid syndrome reveals that genotoxic stress suppresses the somatotroph axis. Nature *444*, 1038–1043.
23. Bardwell, A.J., Bardwell, L., Tomkinson, A.E., and Friedberg, E.C. (1994). Specific cleavage of model recombination and repair intermediates by the yeast Rad1-Rad10 DNA endonuclease. Science *265*, 2082–2085.
24. O'Donovan, A., Davies, A.A., Moggs, J.G., West, S.C., and Wood, R.D. (1994). XPG endonuclease makes the 3′ incision in human DNA nucleotide excision repair. Nature *371*, 432–435.